UCRL 3991

UNIVERSITY OF CALIFORNIA

Radiation Laboratory

BERKELEY, CALIFORNIA

DISCLAIMER

DEFORMATION ENERGY OF A CHARGED DROP. III. FURTHER DEVELOPMENTS

Wladyslaw J. Świątecki*

INTRODUCTION

A theory of any dynamical process is based on the Hamiltonian associated with the system under consideration. For any nuclear phenomenon, including nuclear fission, the Hamiltonian is a many-body expression with complicated and imperfectly known interparticle forces. Some progress in understanding nuclear fission may be made by replacing this complicated Hamiltonian with a simple expression, namely that belonging to a uniformly charged liquid drop, and studying--instead of the theory of the fission of a nucleus--the theory of the fission of such a drop.

The Hamiltonian of a drop, considered as a dynamical system, consists of two parts, the potential and kinetic energies associated with a given deformation, $H = V + T$. A prerequisite for a theory of the division of a drop is an adequate knowledge of V and T in the relevant regions of the deformation space.

This paper is an introduction to a discussion of certain aspects of the many-dimensional "maps" of the potential energy V, considered as a function of the deformation coordinates. Such maps have been studied in the past on several occasions. In the course of a more recent attempt some unexpected, though elementary, features of the problem have come to light, which have suggested the need for a more comprehensive approach in the discussion of the disintegration of a charged drop. In the present studies such a more general approach will be attempted.

Two features of the potential-energy maps (which are themselves functions of the fissionability parameter x, specifying the amount of charge on the drop) follow from elementary considerations. First, the spherical shape is a configuration of equilibrium and, for $x < 1$, there exists a potential energy "hollow" corresponding to the stability of the spherical shape against all small distortions. Second, for very large distortions, by which we mean configurations of separated fragments, there must be a number of potential-energy "valleys," each valley corresponding to a given number of equal fragments separating to large distances. These valleys are discrete in the sense that going from one valley to another requires the surmounting of configurations of

*Radiation Laboratory, University of California, Berkeley, California.

relatively higher potential energy. For example, in order to convert the configuration of two fragments at infinity to a configuration of three fragments at infinity one must, in general, go over intermediate configurations of higher energy. This is analogous to the familiar barrier (a saddle-point pass) that separates the configuration of one fragment (the original sphere) from the configuration of two fragments at infinity. The suggested appearance of the potential energy map is then that of a number of valleys separated from one another by a number of barriers and saddle-point passes.

The depth of the bottom of a valley below the level of the original hollow corresponds to the energy released in the division of the drop into the corresponding number of fragments. The number of valleys for which energy is released increases with x. The general formula for the energy difference between n equal fragments at infinity and the original drop is

$$\frac{\Delta V_n}{E_s^{(0)}} = (n^{1/3} - 1) + 2x\left(\frac{1}{n^{2/3}} - 1\right), \qquad (1)$$

where

$$x = E_c^{(0)}/2E_s^{(0)} = \frac{Z^2/A}{(Z^2/A)_0},$$

with $(Z^2/A)_0 \sim 50$ for a nucleus.

The quantities $E_c^{(0)}$ and $E_s^{(0)}$ are the electrostatic and surface energies of the original drop.

The above energy differences are plotted in Fig. 1 as functions of x for several values of n. A scale of x from 0 to 1 is given as well as an illustrative scale of Z^2/A from 0 to 50. The energy is given in units of $E_s^{(0)}$ and also in Mev, for a nominal value of $E_s^{(0)}$ equal to 700 Mev.

At x = 0 the positive values of ΔV_n correspond to the energy that must be supplied to an uncharged drop to accomplish division. As the charge on the drop is increased division into two equal fragments begins to release energy for $x > 0.35121$. Soon after, divisions into three and four equal fragments become exothermic, and by the time x=0.71 is reached (corresponding to nuclei in the neighborhood of uranium) divisions into five, six, seven, eight, and nine fragments also release energy. Up to $x = 0.61098$ ($Z^2/A = 30.5$), division into two fragments releases the most energy. Beyond this point and up to $x = 0.86502$ ($Z^2/A = 43.3$) division into three fragments takes over first place and division into two fragments falls to second, third, and fourth places. At $x = 0.86502$ division into four fragments begins to

release most energy and continues to do so up to x = 1.11726 ($Z^2/A = 55.9$). At x = 1, the critical value at which the sphere first becomes unstable against small spheroidal distortions, the placing is: 4, 5, 3, 6, 7, 8, 2, 9, 10, ... 20. Two is in seventh place. Configurations of up to 20 fragments at infinity have energies below the energy of the original sphere.

The amount of energy released does not, of course, by itself determine the outcome of the complicated dynamical process of an actual disintegration of a drop, whether into two, three or more fragments, but the following interpretation of the general appearance of Fig. 1 has suggested itself. For a low charge on the drop, when the surface energy is relatively most important, a division into the lowest number of fragments is favored. As the charge is increased and economies in the surface energy become less important in relation to the release of electrostatic energy, divisions into more and more fragments come up for consideration. For some sufficiently high charge, when the electrostatic energy release becomes the dominant factor, one would eventually arrive at a situation where the drop would disintegrate in a violent manner into a large number of fragments (a phenomenon that, under suitable conditions, may be observed when a condenser is suddenly discharged through a droplet of water).*

In connection with Fig. 1, one may also remark that the spherical configuration of a charged drop is an extraordinarily stable one in the sense that it remains a local energy minimum long after it has ceased to be an absolute minimum (at $x \geq 0.35121$, when two separated fragments have a lower energy), and when it finally does become unstable at x = 1, sufficient charge has been accumulated to make a division into as many as 20 fragments exothermic. This situation at x = 1 may be contrasted with the conditions for x around 0.4 when, of the cases shown in Fig. 1, division into two fragments is the only one that releases energy.

A second elementary way of exhibiting the qualitative change in the energy relationships of a disintegrating drop as the charge is increased from relatively low values towards x = 1 is to plot the energy of a drop as a function of a spheroidal distortion. Figure 2 shows the deformation energy $\Delta V/E_s^{(0)}$ as a function of the ratio of the major axis to the minor axis of a spheroid, calculated according to the formula

---

*In practice it is better to use a globule of a conducting liquid suspended in an insulating medium of the same specific gravity. I am grateful to Knud Oleson of the Institute of Physics, Aarhus University, Denmark, for beautiful demonstrations of such disintegrations.

$$\frac{\Delta V}{E_s^{(0)}} = \left\{ \frac{1}{2}\,(1-e^2)^{1/3} \left(1+\frac{\sin^{-1} e}{e\sqrt{1-e^2}} \right) - 1 \right\} +$$

$$+\ 2x \left\{ \frac{1}{2}(1-e^2)^{1/3} \cdot \frac{1}{e}\, \ell n \left(\frac{1+e}{1-e} \right) - 1 \right\}, \qquad (2)$$

where e = eccentricity = $\sqrt{1-(a^2/c^2)}$, and a, c = minor and major semi-axes, respectively.

The different curves in Fig. 2 refer to different values of x. At the lower x values the drop is stable against spheroidal distortions of any magnitude, but as x approaches 1 very elongated shapes become energetically available. The interpretation again suggests itself that with increasing x a transition takes place from conditions governed largely by the stabilizing influence of the surface tension towards an explosive situation associated with the predominance of the electrostatic repulsion. The special stability of the spherical shape is once more in evidence in the fact that by the time the barrier against small deformations finally vanishes at x = 1, violently distorted shapes--like the spheroid with an elongation of 10 to 1--are already available energetically.

Returning to the consideration of the energy releases plotted in Fig. 1, it would be necessary, strictly speaking, to include in a comprehensive account of the fission of a drop a discussion of the role played by the different modes of division as soon as they became energetically available with increasing x. So long as a new division mode is only barely possible there would be some justification in disregarding it in favor of the more exothermic alternatives. As far as Fig. 1 is concerned there is, however, little justification at x values around 0.7 to 0.8 for singling out for consideration the division into two fragments. There is even less justification for this in the case of x close to 1, when divisions into up to 8 fragments release more energy than a division into two. In this connection we note also that the geometrical appearance of the saddle-point shape for x greater than about 0.75--i.e. near spherical for $x \sim 1$ and cylinderlike for $x \sim 0.75$ (see Fig. 8, ref. 2) --offers no hint as to the number of fragments into which the drop might divide after passage of the saddle in the potential energy barrier. In other words, as far as the saddle-point shape is concerned, the drop is not yet "committed" on the question of how many fragments will be formed. Only as x decreases below about 0.7 does the saddle-point shape begin to suggest a more and more pronounced commitment to a division into two fragments, in general accord with the emergence of a preference for such a division at low x values, discussed in connection with Fig. 1

The conclusion suggested by the above discussion is that drops with x values in the neighborhood of 0.7 to 0.8, corresponding to heavy

nuclei, should perhaps be regarded as being in a transition region, somewhere between the situation where a division into only two fragments might be expected, and a region where a more explosive disintegration takes over. In particular, Figs. 1 and 2 suggest that at x=1 the possibility of a rather well-developed situation of the latter kind has to be kept in mind.

Where, precisely, the region of x = 0.7 to 0.8 is located in relation to the two limiting situations is a quantitative question, and so also is the question as to the number of fragments that may be expected to be produced in a disintegration of a drop with some given value of x. For values of x in the neighborhood of 0.5 or higher the answer is not obvious on qualitative grounds, and no quantitative investigations of this problem are available in the published literature. There would appear to be at present no justification for confining the discussion of the fission of a drop, whose charge approaches the limit for the stability of the spherical form, to a consideration of divisions into two fragments only. Indeed, keeping in mind Fig. 2, it would appear that at x ~1, when long cylinderlike configurations are accessible, several possibilities might be available for reassembling such a cylinder into different numbers of fragments. The reassembly could be effected by rippling the surface of the cylinder with an appropriate number of constrictions and then proceeding with the over-all elongation. The process might bear some resemblance to the disintegration of a jet of liquid into separate droplets, considered in connection with fission by Hill and Wheeler,[4] and in connection with jets of water in many classical investigations.[6]

We may note that if we classify the different types of axially symmetric ripples superimposed on a spheroidal surface according to the number r of nodes that they introduce (i.e., according to a quantity related to the average wave length of the ripple), with r an even number for reflection symmetric ripples and odd for asymmetric ripples, then r = 0 is excluded on account of volume preservation and r=1 is excluded if we keep the center of mass fixed. A ripple with r=2 could be taken to correspond to an over-all elongation or contraction of the spheroid, and if this is adopted the dependence of the energy on a distortion of this type would be qualitatively as in Fig. 2. The next case, r = 3, introduces a single waist asymmetrically on one side of the median plane and this, if carried sufficiently far, divides the drop into two unequal fragments. Reversing the sign of the amplitude of the ripple would produce the mirror image of the configuration. The case r = 4 would lead to one waist at the center (and so to a division into two equal fragments) if taken with one sign, or to two waists and three fragments (two of them equal) if taken with the opposite sign. Similarly, for any given r, the ripple would tend to produce a reflection-symmetric string of fragments, $\frac{1}{2}$ r or $\frac{1}{2}$ r + 1 in number, depending on the sign of the ripple. Any odd r would tend to produce an asymmetric string of (r + 1)/2 fragments.

For sufficiently high values of r the increase in surface energy associated with such ripples would make the energies of the corresponding shapes excessively high, so that for any given x one would expect the configurations with a relatively small number of ripples to be the most easily accessible ones.

In view of our previous discussion of Figs. 1 and 2 it would appear that, except at low values of x, it is necessary to investigate the role played by at least a few of the lowest types of ripples. In terms of the potential-energy valleys associated with divisions into different numbers of fragments, the possibility would have to be investigated that, at x values not too far below 1, several of these valleys might be accessible, with the corresponding saddle-point passes at energies relatively low or negative with respect to the spherical configuration.

In available studies of the potential-energy surfaces of charged drops with x values usually in the neighborhood of 0.75, no evidence for the existence of several distinct saddle point passes is apparent (except for certain of the results of Frankel and Metropolis,[12] which could be considered as providing some indirect evidence). It should be borne in mind, however, that in all existing studies of the problem attention was focused on the neighborhood of one definite saddle point, namely that associated with the barrier determining the stability of the spherical form, and no systematic search for other shapes of equilibrium--especially of a more elongated kind--has been described in the published literature.

At very low values of x the existence of many discrete equilibrium configurations, or saddle-point shapes, is indeed well known, a limiting case for $x \to 0$ being axially symmetric configurations of different numbers of equal spherical fragments in contact. The energies of these saddle-point shapes are so far known only for small x, in which case the first one or two powers in an expansion in x are readily calculated. We find, to first order in x, the general formula

$$\frac{\Delta V_n}{E_s(0)} = (n^{1/3}-1) + 2x\left\{\left(\frac{1}{n^{2/3}}-1\right) + \frac{5}{6}\,\frac{1}{n^{5/3}}\left[\frac{1}{n-1} + \frac{2}{n-2} + \frac{3}{n-3} + \right.\right.$$

$$\left.\left. + \ \ldots \ \frac{n-2}{2} + n-1\right]\right\} + \ldots . \qquad (3)$$

The second term in the braces represents the mutual electrostatic energy of n tangent spheres. (Compare the discussion of the case n=2 in Reference 5.) These energies are plotted in Fig. 3, where the energy of the conventional saddle-point shape is also shown (see Ref. 2).

The question of the relation of these families of equilibrium shapes to the rippled cylindrical figures conjectured as possible saddle-point shapes marking the entrances to the different valleys for larger values of x will be taken up presently. We conclude this introduction with two remarks.

First, there exists at the present time no theory of the fission of an idealized liquid drop, not even as regards the broadest qualitative features. Second, there would appear to be more "structure" in the problem than is implied by conventional presentations, essentially because of the possibility that a drop with a charge approaching the critical value for the instability of the spherical configuration might have to be regarded as being in a transitional region of charge values, on the way towards a type of disintegration more drastic than a simple division into two parts.

QUALITATIVE CONSIDERATIONS

In this section we attempt to gain insight into the general features of the potential-energy map relevant to the disintegration of a charged drop by way of elongated, axially symmetric configurations. We make use of qualitative arguments, supplemented by the fragmentary quantitative results available at present. These are mostly for rather small distortions of the drop (the region of the potential-energy hollow around the spherical configuration and the associated barrier and saddle-point shape) and for very large distortions (the valleys corresponding to separated fragments). In the intermediate region we have available the family of spheroidal shapes whose energies are known exactly, and which we shall use as a backbone in our attempt to elucidate the qualitative features of the intermediate region, in particular the way in which the valleys at large distortions somehow come together and then are joined to the conventional saddle-point pass leading out of the spherical configuration. We would like to stress at the outset that this problem is still unsolved, and the speculations described in this section are in no sense implied to constitute a solution; the answers to the many questions involved will be provided only by a satisfactory quantitative treatment.

In order to plot the potential energy of a distorting drop an infinitely many-dimensional map would be required. We shall attempt to illustrate our discussion of the potential energy of axially and reflection-symmetric shapes by sketches in two dimensions, using two coördinates labeled "a_2" and "a_4". The origin, "a_2" = 0 and "a_4" = 0, is taken to correspond to the spherical shape, and for small values of these parameters they may be interpreted quantitatively as the coefficients of P_2 and P_4 in an expansion of the surface of the drop in Legendre polynominals. For larger distortions only a qualitative correspondence with the Legendre polynomials is implied, and for very large distortions, when separate fragments are beginning to

form, these coördinates should be imagined as going over into some suitable set capable of describing such shapes.

A spheroid of a given eccentricity when expanded in Legendre polynomials defines a certain set of coefficients a_2, a_4, ..., and the family of spheroidal distortions of increasing elongation would appear as a curve in the a_2, a_4 diagram as indicated in Fig. 4. The energy of a drop with $x < 1$ distorting along this curve increases for small elongations and may then go through a maximum, followed by a minimum, if the value of x is sufficiently close to 1 (see Fig. 2). In any case, for a sufficiently large elongation the total energy is an increasing function of the elongation, corresponding to the fact that the electrostatic repulsion tending to increase the elongation is finally exceeded by the opposing tendency of the surface tension.

In order to proceed with the division, one of several courses is open to the system: introduction of one or more constrictions in the spheroid decreases the surface tension around the perimeter of the neck or necks, and if the constrictions are sufficiently deep the surface tension is unable to withstand the electrostatic repulsion, further elongation of the system is possible, and the drop can proceed towards division into a number of fragments. In other words, as the constriction or constrictions are deepened the initially positive gradient of the energy with respect to elongation (i.e., the tendency for the spheroid to contract) changes sign and gives place to a negative gradient (tendency to increase the elongation).

In order to translate the above physical considerations into a qualitative potential energy map in the "a_2", "a_4" diagram, consider first the case when just one constriction is introduced halfway across the spheroid. This corresponds to moving away from the "curve of spheroids" in Fig. 4. More specifically, it follows from the geometry of distortions of the type of P_2 and P_4 that the motion is in a general direction of decreasing "a_4" and increasing "a_2," i.e., into a region below and to the right of the curve of spheroids in Fig. 4. If this deviation is continued sufficiently far the total energy should become a decreasing function of the over-all elongation, corresponding to the breaking up of the drop into two separating fragments. We have indicated this in Figs. 4 and 5 by sketching in, below the curve of spheroids, a valley presumed to lead to the two-fragment valley known to be present at large distortions.

Consider now the case in which the amount of "a_4" is increased, i.e., one moves away from the curve of spheroids in an upward direction. Geometrically this corresponds to introducing two constrictions situated symmetrically on either side of the median plane of the spheroid. If this distortion is carried far enough the energy should again become a decreasing function of the elongation and the system should be able to divide into three fragments. We have indicated this by sketching in the three-fragment valley in the upper part of Figs. 4 and 5.

Proceeding to greater elongations and introducing a larger number of constrictions, we could similarly sketch in the valleys leading to divisions into four or more fragments, although there would be need for more than two dimensions in the plots of the maps. In Fig. 5 we have made an attempt to indicate the four-fragment valley by imagining part of the diagram to refer to deviations from the line of spheroids in a new dimension.

The over-all picture implied by these considerations is of a number of valleys, corresponding to disintegrations into different numbers of fragments, clustering around the locus of elongated, cylinderlike shapes along which the drop is still undecided as to how many fragments will be produced.

The low regions in Fig. 5 are shown separated from one another by regions of high potential energy, so that the crossing from one valley to another involves passage over a saddle in the energy. Three such saddle points appear in Fig. 5, separating the configuration of one fragment from that of two, two from three, three from four. Thus the least energy necessary to convert a configuration of one fragment into two fragments at infinity would be the threshold energy corresponding to the conventional saddle point A, whereas the least energy for conversion of two fragments into three would be the energy of the saddle point B, and so on. The geometrical appearance of the saddle-point shape A is known for $x \gtrsim 0.6$ (Fig. 8 in Ref. 2). It represents a balance between the tendency for further elongation and the tendency to return to the spherical shape. According to our qualitative discussion we would expect the saddle-point shape B to be in the general form of an elongated figure with two necks, the amount of necking and the proportions of the figure being adjusted so that there is a balance between the tendency of the drop to disintegrate further into either two or three fragments and the tendency for the system to return to the spherical shape. Similarly the saddle-point shapes marking the entrances to the n-fragment valleys would be expected to be in the general form of rippled cylindrical figures with proportions adjusted to ensure an (unstable) equilibrium with respect to different types of disintegration as well as with respect to a return to a spherical shape.

As regards the dependence of these saddle point shapes on x, it has usually been assumed that, for $x \ll 1$, the saddle-point shape A goes over into the configuration of two equal tangent spheres. More generally we might expect that since the disruptive tendency of the electrostatic repulsion decreases with decreasing x, the necking in for any one of the rippled saddle-point shapes would have to be carried further, as x decreased, before a balance could be achieved between the surface tension and the electrostatic repulsion.

The above qualitative features are indeed exhibited by the familiar saddle-point shapes for $x \ll 1$ mentioned in the Introduction, and we shall eventually assume that the rippled cylindrical figures of

equilibrium introduced in Fig. 5 go over with decreasing x into these configurations of spherical fragments joined by small necks. At present this has not, however, been established by actual calculations over the intermediate values of x. (In particular the relation of the conventional threshold for $x \to 1$ to the threshold associated with $n = 2$ for $x \ll 1$ has not been established).

In order to gain some further insight into the possible appearance of these less familiar saddle-point shapes with many necks we may note that the family of an infinite number of spherical fragments in contact is also a limiting member of the family of axially symmetric surfaces of constant total curvature, familiar in the theory of soap films. (See, for example, Ref. 6.) These surfaces, the "unduloids", may be generated by the curve traced out by a focus of an ellipse imagined to be rolling along the axis of symmetry. The configuration of tangent spheres in contact results when the ellipse is made to degenerate into a straight line joining its foci. It is further shown in the above reference that the longitudinal tension that a liquid surface in the form of an unduloid is capable of supporting is proportional to the square of the minor axis of the ellipse. In an elongated charged figure in the general form of an unduloid, the longitudinal tension due to the electrostatic repulsion would be greatest in the middle and would fall off towards the tips. This suggests that a qualitative picture of the rippled saddle-point shapes discussed previously is perhaps provided by a figure traced out by a focus of an ellipse imagined to be rolling on the axis of symmetry, the ellipse becoming gradually slimmer as the ends are approached and degenerating finally into a straight line when tracing out the tips of the figure.

Concerning an estimate of the threshold energies associated with the above saddle-point shapes, we may add the following remarks to the formula for $x \ll 1$ given in the Introduction (Eq. (3)). The approximation represented by that equation and plotted as the straight lines in Fig. 3 corresponds to assuming the saddle-point shapes to be strings of equal tangent spheres and increasing the charge on them without allowing the shapes to adjust themselves under the influence of the electrostatic repulsion. An estimate of the effect of a readjustment was made by a calculation to the next order in the expansion in powers of x, using a crude variation method in which the shape was assumed to be in the form of spherical fragments joined by small cylindrical necks and the total energy was made stationary with respect to the radii of the fragments as well as the radii and lengths of the necks. The effect of the readjustment was to lower the thresholds, as indicated by the last term in the resulting expansions in the cases for $n = 2$ and $n = 3$:

$$\left.\begin{aligned} \frac{\Delta V_2}{E_s^{(0)}} &= 0.259921 - 0.215112x - 0.219x^2 + \dots \\ \frac{\Delta V_3}{E_s^{(0)}} &= 0.442250 - 0.370792x - 0.213x^2 + \dots \end{aligned}\right\} \qquad (4)$$

For n = 2 the deformation energy is plotted in Fig. 6 as a function of the two available parameters, the separation between the fragments (or, equivalently, the length ℓ of the neck) and the radius r of the neck. The saddle occurs when the length of the neck is equal to its diameter, which, in units of the radius of the original spherical drop, is given by

$$\frac{2r}{R_0} = \frac{\ell}{R_0} = (5/6)\, 2^{2/3}\, x + \ldots .$$

A departure from the saddle shape in the sense of an increased ℓ and a decreased r leads to the two-fragment valley, whereas a decrease of ℓ and an increase of r would make the fragments coalesce and lead back to the spherical shape (see Fig. 6).

For n = 3 the saddle configuration occurs when the radius of the inner fragment exceeds very slightly the radius of the outer ones:

$$(r_{\text{inner}} - r_{\text{outer}})/R_0 = (35/432)3^{2/3}\, x + \ldots ,$$

and the connecting necks have length equal to diameter, as before, (but with $2r/R_0$ equal to $(25/54)3^{2/3}x$). Departures from the saddle shape could lead to one, two, or three fragments.

The small-x approximations to the thresholds (Eq. (4)) are shown in Fig. 3.

For larger values of x no calculations of the thresholds in question are available for $n > 2$. In so far as the saddle point shapes may be in the general neighborhood of elongated cylinderlike configurations, estimates of the energies of such configurations are of interest. In Fig. 7 the energies of spheroids of various eccentricities (the same as in Fig. 2) are plotted against x and the trends are compared with the trends in the thresholds for $x \ll 1$. In Fig. 8 a similar comparison is made for estimated energies of cylinders with hemispherical ends.

The above estimates are quite inadequate to answer quantitatively the important question of the relative order of the threshold energies for any given value of x, except when x is small. It would seem, however, that with increasing x one or more of the thresholds for $n > 2$ might cross and fall below the conventional threshold (n = 2) paralleling perhaps in a general way the crossings that occur in the plot of the relative energy releases in Fig. 1, since both Fig. 1 and Figs. 7 and 8 reflect the tendency towards divisions into more and more fragments with increasing x. With reference to the map in Fig. 5 this would appear as an over-all sinking of the energies of the more elongated configurations represented by the central and upper-right-hand portions of Fig. 5. As a result of this sinking the energies of one or more of the saddle points B, C, ... could fall below the level of the conventional saddle point A. A situation of special interest would occur

if one or more of these crossings of thresholds took place before x reached the value 1. In that case a drop distorted away from the spherical shape to just beyond the first threshold A would still not be committed energetically to a division along the two-fragment valley, but would have available a choice of several valleys, the number of possibilities depending on how many of the other saddle points lay at energies below that of A. In such circumstances the process of fission of a drop would have to be regarded as of a higher order of complexity, in the sense of involving the competition between several distinct modes of disintegration.

With decreasing x the energies of the relatively more elongated shapes would increase relatively more rapidly than the energy in the immediate neighborhood of the spherical configuration and the elongated saddle shapes would successively exceed the energy of A and the associated n-fragment valleys would, one by one, cease to be available (at least as far as low-energy disintegrations are concerned in which only just enough energy is provided to overcome the threshold A). In this way the qualitative circumstances of disintegrating drops would experience an abrupt change every time an intersection occurred between two threshold curves in a plot against x of the type attempted in Figs. 3, 7, and 8. Below some critical value of x where the last such intersection occurred, the two-fragment valley would presumably be the only available one.

When the potential-energy map is translated back into physical considerations, the situation implied is as follows. The possibility of a division of a drop into a given number of fragments should be regarded as being governed by the magnitude of the elongation of a cylinderlike configuration which is accessible for a given charge on the drop and at a given energy. Up to a certain value of the charge, configurations sufficiently elongated to make the introduction of two waists favorable are not accessible (at energies corresponding to the conventional threshold). A drop elongated to beyond the conventional saddle point has then no alternative but to introduce one waist and divide in two.

As the charge is increased, however, there will come a point at which the drop may continue its elongation beyond the conventional saddle point without introducing a waist (and so committing itself to a division in two) and in this way reach a cylinderlike configuration long enough to make the introduction of two waists favorable. In these circumstances two alternatives are open to a dividing drop: after the initial elongation away from the spherical shape the drop may either begin to neck in at relatively moderate elongations towards a dumb-bell configuration, or it may go on with the elongation and then neck in along two waists towards a three-fragment configuration. At higher charges (or, for a given charge, at higher energies) the alternative of still greater elongations, at which the introduction of three or more necks is favorable, would become accessible.

We note here a characteristic difference between the above considerations and the classical discussion of the disintegration of an uncharged (or slightly charged) cylinder of liquid into separate droplets. In the latter case the cylinder is unstable against ripples whose wave length exceeds the circumference of the cylinder,[6] but the configurations of disintegrated fragments are not associated with discrete potential-energy valleys. The only true energy minimum is that associated with the configuration in which all the liquid is reassembled into a single sphere and the energy of any other configuration, like that of two fragments, may be decreased continuously towards this minimum (by the transfer of material from one fragment to the other). The observed disintegration of a cylinder or jet of water into a more or less characteristic number of droplets per unit length of jet is the result of dynamical aspects of the situation, involving the competition between the increasing instability against ripples of increasing wave length and the increasing inertia involved in the reassembly into large drops (consult Ref. 6). On the other hand, in the case of a sufficiently charged drop, there exist definite potential-energy valleys associated with divisions into two, three, or more fragments (Fig. 1), and, apart from dynamical considerations, the potential energy itself already shows preferences for divisions into certain numbers of fragments. The more complex structure of the potential energy map shown in Fig. 5, exhibiting several valleys and thresholds, is associated with the presence of a charge on the drop.

In Figs. 9(a), 9(b), and 9(c) an attempt is made to illustrate the conditions on the two sides of a critical x value at which there occurs a crossing between two threshold-energy curves. For purposes of illustration we have assumed that the crossing takes place at a value x_1 less than unity between the thresholds for n = 2 and n = 3. (This could be the last crossing to occur with decreasing x.)

In Fig. 9(a), representing the case for $x > x_1$, both the two- and three-fragment valleys are energetically available and an actual disintegration of a drop would involve a competition between two modes, one associated with the two-fragment valley and the other with the three-fragment valley. In this connection it may be noted that the fact that the deforming drop has entered the three-fragment valley does not necessarily mean that the final result of the disintegration will be three fragments. For this to be the case one would have to ensure, in addition, that after entering the three-fragment valley by way of some two-necked saddle-point shape B, the deformation proceed in a manner sufficiently symmetric as regards the further necking in of the two constrictions to lead to a breaking off of both end fragments. If this condition were not satisfied the result would still be two fragments, in general unequal in size. It might be that an actual division into three fragments would begin to occur with appreciable probability only for x values significantly in excess of the minimum value where the three-fragment valley first became energetically available, i.e., only after the energetic advantages of a

division into three fragments had been able to assert themselves in a sufficiently decisive manner. In a range of x values only moderately in excess of the minimum, the conditions for a sufficiently simultaneous breaking off of the two necks might be satisfied but rarely, and after the severance of one neck the remainder of the drop, representing a system with a smaller ratio of electrostatic to surface energy, might fail to complete division, thus remaining as a single relatively large fragment. (For example, if a fraction k of a drop with a uniform charge corresponding to a value x is broken off, the remainder is characterized by a new x value given by $(1-k)x$. With $x = 0.75$ and $k = 1/3$, this would give $x_{new} = 0.5$. As suggested by Fig. 8 of Ref. 2, the distortion necessary to carry such a fragment over the barrier against further division is considerable, and in cases where the necking in was less advanced the fragment would in general remain undivided. (Compare the similar discussion in Ref. 4.) The possibility should be kept in mind that, in effect, the competition between the two-fragment valley and the three-fragment valley might be, under certain circumstances, a competition between a symmetric and an asymmetric division mode.

Similarly, divisions that make use of the n = 4, 5, 6, ... valleys need not necessarily lead to disintegrations into four, five, six, ... fragments, but could produce a variety of results, depending on the value of x and the dynamic aspects of the process. (This is not to say that each mode would not be associated with more or less characteristic features that would distinguish it from divisions proceeding by way of other valleys.) The probability of an actual division into three or more fragments would be expected to increase with x.

Returning to Figs. 9(a) to (c), we note the sudden qualitative change in the conditions governing the disintegration of the drop as x falls below x_1. Whereas for $x > x_1$ the disintegration would be the result of a competition between two qualitatively different modes, for $x < x_1$ the system is suddenly forced on energetic grounds to go entirely by way of the two-fragment valley, at least in cases in which only just enough energy is available to carry it over the first saddle point A. (With increasing energy the characteristics of a competition would reappear when the threshold B was exceeded.)

The possible occurrence of such discontinuous changes even within the framework of a classical model of an idealized drop is a feature which should, perhaps, be taken as an indication of the richness of hitherto unexplored phenomena that may be revealed in a thorough quantitative study of the oscillations and disintegration of a charged liquid drop.

The foregoing discussion of the potential-energy map has been confined to elongated, axially symmetric shapes. We shall not attempt to discuss systematically the more general cases, but we may note that there certainly exist many other shapes of equilibrium of a

charged drop. Examples that suggest themselves are oblate and ring-shaped configurations; families of equilibrium shapes that degenerate into the sphere at the higher x values, at which the sphere loses stability against distortions proportional to the higher spherical harmonics (some of these may be related to the shapes we have discussed); configurations in the form of a thick spherical shell with a hollow center (see Ref. 11); and nonaxially symmetric shapes, of which a limiting form for $x \to 0$ would be, for example, a set of three equal tangent spheres with triangular symmetry, joined by small necks.

One special class of equilibrium shapes whose existence may be of some significance, at least for questions of principle, consists of numbers of unequal, separated spherical fragments. For two equal fragments at infinity the total energy is always stationary with respect to changes in all parameters specifying the configuration, including a change in the relative size of the fragments. If the charge is sufficiently high ($x > 1/5$) there exists, in addition, a configuration of two unequal fragments whose energy is stationary, being a maximum with respect to a change of relative size. The significance of these new saddle-point configurations is in part related to the definition of the conventional threshold energy as the least energy necessary to divide a drop in two. It is clear that to divide a drop into very unequal parts requires only a small amount of energy, unrelated to the conventional threshold. In fact, for a vanishingly small fragment, this energy becomes equal to the surface energy of the new droplet formed, the change in the electrostatic energy being of higher order in the droplet size. As the new fragment increases and the release of electrostatic energy compensates the increase in the surface, the total energy of two such fragments at infinite separation goes through a maximum and then decreases towards the negative value associated with the energy release in a division into equal parts. The energy at the maximum -- the threshold associated with the new saddle-point shape mentioned above -- is the least energy required to divide a drop into comparable parts by a sequence of configurations in which a very long and thin filament, of negligible energy, is first emitted and then matter is transferred along this filament to a spherical swelling at its far end. The threshold for this type of division is compared with the conventional threshold in Fig. 10. For $x < 0.724$ a drop could be divided into two comparable fragments using less energy than the conventional threshold energy.

The existence of a maximum in a plot of the energy of two sufficiently charged fragments against the ratio of their sizes suggests the possible existence of yet another family of equilibrium configurations. For two fragments not at infinity but at some finite separation; their energy is modified by their mutual interaction. An example is the familiar case of (unequal) tangent spheres whose energy for different values of x has been plotted in Fig. 9 of Ref. 12. As before, and essentially for the same reasons, there exists, for

a sufficinetly high charge ($x > 3/5$), a maximum in the energy for unequal fragments, as well as a minimum for equal fragments. These configurations however, are no longer equilibirum shapes, because the energy is not stationary with respect to a separation of the fragments under the influence of the electrostatic repulsion. On the other hand, if a pair of fragments is brought into still more intimate contact by establishing a neck of matter between them -- i.e., deforming the system towards the configuration of an undifferentiated drop -- the electrostatic repulsion may be overcome by the surface tension, and the fragments, instead of separating, coalesce. This suggests that starting with any given ratio of sizes of fragments the energy would possess a maximum as a function of a separation coordinate for some intermediate degree of differentiation of the fragments. (This is essentially the same as saying that in the course of the removal of some given amount of matter from a charged drop the potential energy will, in general, go through a maximum.) Since, as we saw, there may exist a maximum also with respect to relative fragment size, the question arises as to the existence, for not-too-small values of x, of an asymmetric figure of equilibirum adjusted in such a way that its energy is stationary (a maximum) both with respect to a change in the degree of differentiation of the fragments and with respect to a change in their relative sizes.

This possibility has been examined by studying the energy of two unequal spheres connected by a cylindrical neck of length ℓ and radius r. When the charge on the drop is low ($x \ll 1$) the neck is small and its electrostatic energy and volume are of higher order than its linear dimensions and its surface area. In this approximation the deformation energy of the system in units of $E_s^{(0)}$ is given by

$$\frac{\Delta V}{E_s^{(0)}} = (U^{2/3} + W^{2/3} - 1) + 2x\,(U^{5/3} + W^{5/3} - 1 + \frac{5}{3}\,\frac{UW}{U^{1/3}+W^{1/3}}) - 2x \cdot \frac{5}{3}\,\frac{UW}{(U^{1/3}+W^{1/3})^2} \cdot \frac{\ell}{R_0} + \frac{1}{2}\left[\frac{r}{R_0} \cdot \frac{\ell}{R_0} - \left(\frac{r}{R_0}\right)^2\right],$$

where U and W are the fractional volumes of the two fragments (U+W=1). The first term contains the surface energy of the fragments, the second the electrostatic energy of touching spheres, the third gives the decrease of the electrostatic energy when the fragments move apart through a distance ℓ, and the last term is the surface energy change due to the neck.

For U = W the above expression may be made stationary for any value of x by a suitable choice of ℓ (=2r). The associated shape is

then an estimate of the symmetric saddle-point shape for $x \ll 1$, as discussed previously.

At the point $x = x_1$, where

$$x_1 = (-12 + 18\sqrt{2})/35 = 0.384452,$$

there occurs a "point of bifurcation," and for $x > x_1$ there exist, in addition to the symmetric one, two reflected asymmetric configurations of equilibrium. The degree of asymmetry of these configurations increases with increasing x in a manner characteristic of such bifurcations, namely proportionally at first to $\sqrt{x-x_1}$. A few illustrations of these shapes are given in Fig. 11 and their energies are plotted in Fig. 10.

The value $x_1 \sim 0.38$ is an estimate, based on a method approximately valid for $x \ll 1$, of the point at which the conventional symmetric saddle-point shape becomes stable against asymmetry: above this value it is "flanked" on either side by an asymmetric shape of equilibrium of higher energy. Conversely, with decreasing x the two "peaks" at asymmetric configurations come together and stability of the symmetric saddle against a symmetry is lost at $x \sim 0.38$. (Compare the trend with x in the stability against asymmetry of the conventional saddle-point shape for $x \to 1$, plotted in Fig. 16.)

The significance of these asymmetric equilibrium shapes has not been investigated, but since they represent a maximum in the energy as regards fragment ratio, they would appear to be associated with particularly unfavored modes of disintegration: for still more asymmetric divisions, like the emission of a small droplet, less energy would be required because the division is then altogether less drastic. For more symmetric divisions better use can be made of the electrostatic repulsion to help the system over the barrier. The above asymmetric shapes of equilibrium might play a role in a discussion of the competition between the many different modes in which an excited drop may dissipate its energy, ranging from the emission of small droplets to more conventional types of fission. Our discussion suggests that, except for small values of x, intermediate modes of disintegration might be expected to be less favorable than either extreme.

The existence of still further configurations of equilibrium of a charged drop, associated with bifurcations along the other families of rippled saddle-point shapes, is suggested by the possibility of adjusting the relative sizes of three or more unequal fragments in such a way that the total energy becomes stationary. The problem exhibits many formal analogies with the classical discussions of the forms of equilibrium of rotating liquid masses, associated with the names of Poincaré, Darwin, Jeans, Liapounoff, and others. (See, for example, Ref. 13).

The above speculations are intended to underline the fact that the discovery, classification, and evaluation of the shapes of equilibrium of a charged drop are at present outstanding unsolved problems in the theory of the disintegration of a liquid drop.

QUANTITATIVE TECHNIQUES

In this part we report some progress towards a quantitative treatment of the problem of a dividing drop. The technique used was an expansion of the shape of the drop about a spheroid, described with the aid of prolate spheroidal coordinates, and the calculation of quantities of interest in powers of the deviation from the spheroid. (Consult Refs. 2, 3, 7, and 8 for such expansions.) Depending on the number of terms retained and the rate of convergence of the expansions, this method should enable one to investigate quantitatively a more or less extensive neighborhood of the curve of spheroids in Fig. 5. Such expansions have proved to be accurate in the neighborhood of the saddle point A, for a range of x values, and if they turn out to be adequate also in the neighborhood of the other saddle points a quantitative treatment of the essential stages in the disintegration of a drop may be feasible along these lines.

It has been found possible to derive general formulae for obtaining expansions of the surface and electrostatic energies of a distorted spheroid of any eccentricity for a general distortion described by an arbitrary number of spheroidal harmonics and to any order in the distortion. We shall summarize some of the results obtained, keeping in mind applications of expansions of this type also to aspects of the problem other than the potential-energy maps. (For example, the study of the dynamics of the disintegration.) We shall present, therefore, not only the final formulae for the potential energies but also an outline of the techniques used in these nth-order expansions, as well as some tables of coefficients, which, being associated with geometrical aspects of a distorted spheroid, would be useful also in more general applications.

1. Volume and Center of Mass of a Distorted Spheroid.

The shape of the axially symmetric drop will be specified in prolate spheroidal coordinates ξ, η, ϕ (see Refs. 2, 9) by giving η as a function of ξ,

$$\eta(\xi) = \eta_0 \left[1 + \sum_{n=0}^{\infty} a_n P_n(\xi)\right] = \eta_0 + \Delta(\xi) = \eta_0 \left[1 + \delta(\xi)\right].$$

The case $\eta(\xi) = \eta_0$ corresponds to a spheroid of eccentricity $e = \eta_0^{-1}$, whose major and minor semi-axes will be denoted by c and a. The volume $V_0 = (4/3)\pi a^2 c$ will be taken equal to the volume $(4/3)\pi R_0^3$ of a sphere of radius R_0. The relation of ξ, η, ϕ to cylindrical polar

coordinates ρ, z, ϕ is

$$\rho = k(1-\xi^2)^{\frac{1}{2}}(\eta^2-1)^{\frac{1}{2}} ,$$

$$z = k\,\xi\,\eta ,$$

$$\phi = \phi .$$

The constant k is half the distance between the foci; $k = ec = \sqrt{c^2 - a^2}$. The lengths of three orthogonal displacements associated with small changes $d\xi$, $d\eta$, $d\phi$ are given by $h_1 d\xi$, $h_2 d\eta$, $h_3 d\phi$, where

$$h_1 = k\left(\frac{\eta^2-\xi^2}{1-\xi^2}\right)^{\frac{1}{2}} ,$$

$$h_2 = k\left(\frac{\eta^2-\xi^2}{\eta^2-1}\right)^{\frac{1}{2}} ,$$

$$h_3 = \rho = k(1-\xi)^{\frac{1}{2}}(\eta^2-1)^{\frac{1}{2}} ; \quad h_1 h_2 h_3 = k^3(\eta^2-\xi^2).$$

The change in volume associated with the distortion $\Delta(\xi)$ is

$$\delta V = \int_{-1}^{1} d\xi \int_{\eta_0}^{\eta_0+\Delta} d\eta \int_{0}^{2\pi} d\phi\, h_1 h_2 h_3$$

$$= 2\pi k^3 \eta_0^{\,3} \int_{-1}^{1} d\xi \left(\delta+\delta^2+\tfrac{1}{3}\delta^3-\eta_0^{\,-2}\xi^2\delta\right) .$$

Integrals of the type

$$\int_{-1}^{1} \delta^r d\xi$$

will occur frequently; we introduce the expansions

$$\delta^r = \sum_{i=0}^{\infty} c_i^{(r)} P_i(\xi) \; ; \qquad c_i^{(r)} = \frac{2i+1}{2} \int_{-1}^{1} P_i \delta^r d\xi .$$

For r = 0:

$$c_0^{(0)} = 1, \qquad c_i^{(0)} = 0 \quad \text{for } i > 0.$$

For r = 1:

$$c_i^{(1)} = a_i .$$

The coefficients $c^{(r+1)}$ can be generated from a recurrence relation obtained as follows:

$$c_i^{(r+1)} = \frac{2i+1}{2} \int_{-1}^{1} d\xi P_i \delta^r \cdot \delta = \frac{2i+1}{2} \int_{-1}^{1} d\xi \, P_i$$

$$\left(\sum_0^\infty c_n^{(r)} P_n \right) \left(\sum_0^\infty a_m P_m \right) =$$

$$\frac{2i+1}{2} \sum_m \sum_n (imn) \, a_m c_n^{(r)} ,$$

where $(imn) \equiv \int_{-1}^{1} d\xi \, P_i P_m P_n$, (see Ref. 2), and the sums $\sum_m \sum_n$ are over all nonvanishing combinations of (imn).

The tabulation of the coefficients $c_i^{(r)}$, defining the expansion of the rth power of

$$\sum_{n=0}^{\infty} a_n P_n$$

is a purely algebraic problem which can be carried out, once and for all, independently of the particular application contemplated. Tables of $c_i^{(r)}$ are given later.

We note the following results:

$$\int_{-1}^{1} \delta^r \cdot P_i \, d\xi = \frac{2}{2i+1} \, c_i^{(r)} ,$$

$$\int_{-1}^{1} \delta^r \cdot \left(\sum_0^\infty a_i P_i \right) d\xi = \sum_{i=0}^{\infty} \frac{2}{2i+1} \, a_i c_i^{(r)} ,$$

$$\int_{-1}^{1} \delta^r \cdot \left(\sum_0^\infty a_i P_i \right) \left(\sum_0^\infty b_j P_j \right) d\xi = \sum_{i,j,k=0}^{\infty} (ijk) a_i b_j c_k^{(r)} .$$

Using these relations, we find for the relative change in volume, $\delta V/V_0$, where $V_0 = (4/3) \pi R_0^3 = (4/3)\pi k^3 (\eta_0^3 - \eta_0)$, the exact expression

$$\frac{\delta V}{V_0} = \frac{\eta_0^2}{\eta_0^2 - 1} \{(3-\eta_0^{-2})\, c_0^{(1)} - \frac{2}{5}\eta_0^{-2} c_2^{(1)} + 3c_0^{(2)} + c_0^{(3)}\} =$$

$$(1-e^2)^{-1} \cdot \{(3-e^2)a_0 - \frac{2}{5}e^2 a_2 + 3\sum_0^\infty \frac{a_n^2}{2n+1} + \tfrac{1}{2}\sum_{p,q,r=0}^{\infty}\sum\sum (pqr)\, a_p a_q a_r\}\,.$$

The special case in which the spheroid degenerates into a sphere corresponds to taking the limit $e \to 0$, $k\eta_0 \to R_0$.

The z coordinate of the center of mass of the distorted shape is given by

$$\bar{z} = \frac{\int_{-1}^{1}\int_{1}^{\eta_0+\Delta}\int_{0}^{2\pi} d\xi\, d\eta\, d\phi\, h_1 h_2 h_3\, z}{\int_{-1}^{1}\int_{1}^{\eta_0+\Delta}\int_{0}^{2\pi} d\xi\, d\eta\, d\phi\, h_1 h_2 h_3}\,.$$

The denominator is the distorted volume $V = V_0 + \delta V$; evaluation of the numerator leads to the result

$$V\bar{z} = \frac{4}{3}\pi R_0^4 \cdot (1-e^2)^{-4/3} \{(c_1^{(1)} + \frac{3}{2}c_1^{(2)} + c_1^{(3)} + \frac{1}{4}c_1^{(4)}) -$$

$$e^2(\frac{3}{5}c_1^{(1)} + \frac{6}{35}c_3^{(1)} + \frac{3}{10}c_1^{(2)} + \frac{3}{35}c_3^{(2)})\}\,.$$

2. The Surface Energy

The surface area of the distorted drop is given by

$$A = \int_{\xi=-1}^{1}\int_{\phi=0}^{2\pi} \sqrt{(h_1 d\xi)^2 + (h_2 d\eta)^2}\, h_3 d\phi =$$

$$2\pi k^2 \int_{-1}^{1} d\xi \sqrt{(\eta^2-\xi^2)\,[\eta^2 - 1 + (1-\xi^2)(d\eta/d\xi)^2]} =$$

$$2\pi R_0^2 \cdot (1-e^2)^{-2/3} \int_{-1}^{1} d\xi \sqrt{(x^2 - e^2\xi^2)(x^2 - e^2 + y)}\,,$$

where

$$x = \frac{\eta}{\eta_0} = 1 + \delta ,$$

$$y = (1-\xi^2)\left(\frac{d\delta}{d\xi}\right)^2 .$$

Considering the integrand as a function of x and y and expanding in a Taylor series about the point x = 1, y = 0 we find

$$A = 2\pi R_0^{\,2} \cdot (1-e^2)^{-2/3} \cdot \int_{-1}^{1} d\xi \sum_{n=0}^{\infty} \sum_{s=0}^{\infty} \frac{\delta^n y^s}{n!\, s!} \left\{ \frac{\partial^{n+s}}{\partial x^n \partial y^s} (x^2-e^2\xi^2)^{\frac{1}{2}} (x^2-e^2+y)^{\frac{1}{2}} \right\}_{\substack{x=1 \\ y=0}} .$$

Introducing the expansions

$$y^s = \sum_{i=0}^{\infty} d_i^{(s)} P_i(\xi) ,$$

$$\left\{ \frac{\partial^{n+s}}{\partial x^n \partial y^s} (x^2-e^2\xi^2)^{\frac{1}{2}} (x^2-e^2+y)^{\frac{1}{2}} \right\}_{\substack{x=1 \\ y=0}} = \sum_{i=0}^{\infty} C_i^{(n,\,s)} P_i(\xi) ,$$

we may write

$$B_s = \frac{A}{4\pi R_0^{\,2}} = \frac{1}{2} \cdot (1-e^2)^{-2/3} \cdot \sum_{n=0}^{\infty} \sum_{s=0}^{\infty} \frac{1}{n!\, s!} \sum_{i,\,j,\,k=0}^{\infty} (ijk)\, c_i^{(n)}\, d_j^{(s)}\, C_k^{(n,\,s)} .$$

The coefficients $d_i^{(r+1)}$ may be calculated in terms of $d_i^{(r)}$ by means of the recurrence relation

$$d_i^{(r+1)} = \frac{2i+1}{2} \sum_{m} \sum_{n} (imn)\, d_m^{(1)}\, d_n^{(r)} .$$

For $r = 0$: $d_0^{(0)} = 1$, $d_i^{(0)} = 0$ for $i > 0$.

In order to find $d_i^{(1)}$ we proceed as follows:

$$d_i^{(1)} = \frac{2i+1}{2} \int_{-1}^{1} d\xi \, P_i \cdot \left((1-\xi^2) \frac{d\delta}{d\xi} \right) \cdot \left(\frac{d\delta}{d\xi} \right).$$

Now we have

$$\frac{dP_i}{d\xi} = (2i-1) P_{i-1} + (2i-5) P_{i-3} + \ldots \quad \text{down to } P_0 \text{ if i odd or to } 3P_1 \text{ if i even}$$

$$\therefore \frac{d\delta}{d\xi} = (a_1 + a_2 + a_4 + \ldots)P_0 + 3(a_2 + a_4 + a_6 + \ldots)P_1 +$$

$$+ 5(a_3 + a_5 + a_7 + \ldots)P_2 + \ldots$$

$$= \sum_{m=0}^{\infty} B_m P_m ,$$

where

$$B_m = (2m+1)(a_{m+1} + a_{m+3} + a_{m+5} + \ldots) ;$$

also

$$(1-\xi^2) \frac{d\delta}{d\xi} = \sum_{n=1}^{\infty} a_n (1-\xi^2) \frac{dP_n}{d\xi} = \sum_{n=1}^{\infty} a_n \cdot \frac{n(n+1)}{2n+1} \cdot$$

$$\times (P_{n-1} - P_{n+1}) = \sum_{n=0}^{\infty} A_n P_n ,$$

where

$$A_n = - \frac{(n-1)n}{2n-1} a_{n-1} + \frac{(n+1)(n+2)}{2n+3} a_{n+1} .$$

Hence the starting values $d_i^{(1)}$ for use in the recurrence relation for $d_i^{(r+1)}$ are found from

$$d_i^{(1)} = \frac{2i+1}{2} \sum_m \sum_n (imn) B_m A_n .$$

The coefficients $C_k^{(n,s)}$ are obtained as follows:

$$\left\{\frac{\partial^{n+s}}{\partial x^n \partial y^s}\ (x^2-e^2\xi^2)^{\frac{1}{2}}\ (x^2-e^2+y)^{\frac{1}{2}}\right\}_{\substack{x=1\\y=0}} = \left\{\frac{\partial^{n+s}}{\partial x^n \partial z^s}\ F(x,z)\right\}_{\substack{x=1\\z=B^2}} =$$

$$= \left\{F_{n,s}\right\}_{\substack{x=1\\z=B^2}} ,$$

where

$$z = 1 - e^2 + y ,$$

$$F^2 = (x^2 - 1 + a^2)(x^2 - 1 + z) = (x^2 - 1)^2 + (x^2 - 1)(a^2 + z) + a^2 z,$$

with

$$a = (1-e^2\xi^2)^{\frac{1}{2}} ,$$

$$B = (1-e^2)^{\frac{1}{2}} .$$

$F_{n,s}$ denotes the nth derivative with respect to x and the sth derivative with respect to z.

Recurrence relations for the successive derivatives of F are obtained by differentiating F^2, equal to G, say. By equating the different powers of x and z in the Taylor expansions of G and F · F we obtain the following relation between the differential coefficients of F and G:

$$\frac{G_{k,\ell}}{k!\,\ell!} = \sum_{m=0}^{k} \sum_{n=0}^{\ell} \frac{F_{m,n}\, F_{k-m,\ \ell-n}}{m!\,(k-m)!\,n!\,(\ell-n)!} \qquad (5)$$

On the left the $G_{k,\ell}$ are simple coefficients of which only a few (with the lowest k and ℓ) differ from zero. Thus, at x = 1, z = B^2, we find

$$G = a^2B^2 ,$$

$$G_{10} = 2(a^2+B^2) ,$$

$$G_{20} = 8 + 2(a^2+B^2),$$

$$G_{30} = 24,$$

$$G_{40} = 24 ,$$

$$G_{01} = a^2 ,$$

$$G_{11} = 2 ,$$

$$G_{21} = 2 .$$

All other $G_{k,\ell}$ vanish.

The right-hand side of Eq. (5) may be regarded as providing a relation between F times the highest occuring derivative of F and the lower derivatives, assumed known. In this way the successive derivatives of F are readily generated.

For example, in an expansion to third order in the coefficients a_i, the six quantities F, F_{10}, F_{20}, F_{30}, F_{01}, F_{11} have to be calculated at $x = 1$, $z = B^2$. We find

$$F = Ba,$$

$$F_{10} = B^{-1}a + Ba^{-1},$$

$$F_{20} = (B^{-1} - B^{-3})\,a + (B + 2B^{-1})\,a^{-1} + (-B)a^{-3},$$

$$F_{30} = (-3B^{-3} + 3B^{-5})a + (6B^{-1} - 3B^{-3})a^{-1} + (-3B - 3B^{-1})\,a^{-3} + (3B)a^{-5},$$

$$F_{01} = \tfrac{1}{2} B^{-1}a,$$

$$F_{11} = -\tfrac{1}{2} B^{-3}a + \tfrac{1}{2} B^{-1}a^{-1}.$$

Making use of the expansions

$$a^r = (1-e^2\xi^2)^{r/2} = \sum_{k=0}^{\infty} D_k^{(r)}\, P_k(\xi),$$

where $D_k^{(r)}$ are coefficients for which recurrence relations are given in Ref. 2, we find

$$C_k^{(0,\,0)} = BD_k^{(1)},$$

$$C_k^{(1,\,0)} = B^{-1}D_k^{(1)} + BD_k^{(-1)},$$

$$C_k^{(2,\,0)} = (B^{-1}-B^{-3})\,D_k^{(1)} + (B+2B^{-1})\,D_k^{(-1)} + (-B)D_k^{(-3)},$$

$$C_k^{(3,\,0)} = (-3B^{-3}+3B^{-5})D_k^{(1)} + (6B^{-1}-3B^{-3})D_k^{(-1)} + (-3B-3B^{-1})D_k^{(-3)} + (3B)\,D_k^{(-5)},$$

$$C_k^{(0,\,1)} = \tfrac{1}{2} B^{-1}\,D_k^{(1)},$$

$$C_k^{(1,\,1)} = -\tfrac{1}{2} B^{-3}D_k^{(1)} + \tfrac{1}{2} B^{-1}D_k^{(-1)}.$$

The higher-order terms are obtained in a similar manner. In this way all the coefficients entering the expansion for the relative surface area (or the relative surface energy B_s) may be calculated by

means of recurrence relations for which general formulae are available for any eccentricity and any distortion specified by

$$\delta = \sum a_n P_n .$$

3. The Electrostatic Energy

The electrostatic energy of a distorted spheroid is given by

$$E_c = \tfrac{1}{2}\rho^2 \int_{-1}^{1} \int_{1}^{\eta_0+\Delta} \int_{0}^{2\pi} d\xi\, d\eta\, d\phi\, h_1 h_2 h_3 \int_{-1}^{1} \int_{1}^{\eta_0+\Delta} \int_{0}^{2\pi} d\xi'\, d\eta'\, d\phi'\, h'_1 h'_2 h'_3 \frac{1}{PP'} ,$$

where PP' is the distance between the points (ξ, η, ϕ) and (ξ', η', ϕ'). Here Δ stands for $\eta_0 \delta(\xi)$ and Δ' for $\eta_0 \delta(\xi')$.

If the distorted shape is considered as made up of two parts, the spheroid and the distortion, we may decompose E_c into three terms:

$$E_c = E_{\text{spheroid}} + E_{\text{distortion}} + E_{\text{interaction}} ,$$

where

$$E_{\text{spheroid}} = \tfrac{1}{2}\rho \int_{\text{spheroid}} v_{\text{spheroid}},$$

$$E_{\text{distortion}} = \tfrac{1}{2}\rho \int_{\text{distortion}} v_{\text{distortion}} ,$$

$$E_{\text{interaction}} = \rho \int_{\text{distortion}} v_{\text{spheroid}},$$

where v_{spheroid}, $v_{\text{distortion}}$ are the electrostatic potentials produced by the parts indicated.

We shall derive a general formula for E_c, using a method outlined by N. Mudd in Ref. 10, according to which the potential of a finite distortion (in regions of space outside the distortion itself) may be represented as a superposition of the potentials due to a series of suitable surface charges.

The potential due to a finite distortion Δ is

$$v_{dist} = \rho \int_{-1}^{1} d\xi' \int_{0}^{2\pi} d\phi' \int_{\eta_0}^{\eta_0+\Delta'} d\eta' \left(\frac{h'_1 h'_2 h'_3}{PP'}\right).$$

Expanding the integrand in a Taylor series and integrating term by term, we find

$$v_{dist} = \rho \int_{-1}^{1} \int_{0}^{2\pi} d\xi' \, d\phi' \int_{\eta_0}^{\eta_0+\Delta'} d\eta' \sum_{p=0}^{\infty} \frac{(\eta'-\eta_0)^p}{p!} \cdot \left\{ \frac{\partial^p}{\partial \eta'^p} \left(\frac{h'_1 h'_2 h'_3}{PP'}\right) \right\}_{\eta'=\eta_0} =$$

$$= \rho \int_{-1}^{1} \int_{0}^{2\pi} d\xi' d\phi' \sum_{p=0}^{\infty} \frac{(\delta')^{p+1}}{(p+1)!} \left\{ \eta_0^{p+1} \frac{\partial^p}{\partial \eta'^p} \left(\frac{h'_1 h'_2 h'_3}{PP'}\right) \right\}_{\eta'=\eta_0}.$$

Mudd's method consists in interchanging the order of integration with respect to (ξ', ϕ') and the differentiations with respect to η':

$$v_{dist} = \sum_{p=0}^{\infty} \frac{1}{(p+1)!} \left\{ \eta_0^{p+1} \frac{\partial^p}{\partial \eta'^p} \int_{-1}^{1} \int_{0}^{2\pi} h'_1 d\xi' h'_3 d\phi' \frac{\rho(\delta')^{p+1} h'_2}{PP'} \right\}_{\eta'=\eta_0}. \quad (6)$$

In so far as this interchange is justified (this question has not been studied adequately) the potential v_{dist} has now been expressed as a sum from p = 0 to infinity of $\eta_0^{p+1}/(p+1)!$ times the pth derivative with respect to η', evaluated at $\eta' = \eta_0$, of the potential of a series of surface charges equal to $\rho(\delta')^{p+1} h'_2$, distributed on a spheroid given

by $\eta' = \text{constant}$.

The general formulae for the internal or external potentials ($v^<$ or $v^>$) at a point η, ξ, ϕ due to any surface distribution of charge σ on a spheroid defined by $\eta = \eta_0$, are given in Ref. 9. (Ch. 5, Problem 89). For example,

$$v^< (\xi, \eta, \phi) = \sum_{n=0}^{\infty} \sum_{m=0}^{\infty} M_{mn} P_n^m(\eta) P_n^m(\xi) \cos m\phi, \tag{7}$$

where

$$M_{mn} = (-1)^m (2-\delta_{m0}) k^{-1} (2n+1) \left[\frac{(n-m)!}{(n+m)!}\right]^2 Q_n^m(\eta_0) \int_{-1}^{1} \int_{0}^{2\pi} P_n^m(\xi)$$

$$\cos m\phi \cdot \sigma \, h_1 h_3 \, d\xi \, d\phi .$$

Here P_n^m, Q_n^m are the associated Legendre polynomials of the first and second kind, respectively. In our case the surface charges are in the form

$$\sigma = \rho h_2 \sum_{n=0}^{\infty} c_n P_n(\xi),$$

so that we have

$$h_1 h_3 \sigma = \rho k^3 (\eta_0^2 - \xi^2) \sum_{n=0}^{\infty} c_n P_n(\xi).$$

Re-expanding, we may write

$$h_1 h_3 \sigma = \rho k^3 \sum_{n=0}^{\infty} X_n(\eta_0, c) P_n(\xi),$$

where the expansion coefficients X_n are related to the c_n through

$$X_n(\eta_0, c) = -\frac{(n-1)n}{(2n-3)(2n-1)} c_{n-2} + \left[(\eta_0^2 - \frac{1}{3}) - \frac{2}{3} \frac{n(n+1)}{(2n-1)(2n+3)}\right] c_n - \frac{(n+1)(n+2)}{(2n+3)(2n+5)} c_{n+2}. \tag{7a}$$

Substitution in Eq. (7) gives

$$v^< (\xi, \eta) = 4\pi\rho k^2 \sum_{n=0}^{\infty} P_n(\xi) \cdot P_n(\eta) Q_n(\eta_0) X_n(\eta_0, c).$$

Applying this result to (6), we find for the inside potential of a finite distortion the expression

$$v^{<}_{\text{dist}}(\eta, \xi) = 4\pi\rho k^2 \eta_0^2 \sum_{p=0}^{\infty} \frac{1}{(p+1)!} \sum_{n=0}^{\infty} P_n(\xi) \cdot W_{np}(\eta_0) \cdot P_n(\eta) ,$$

where

$$W_{np}(\eta_0) = \left\{ \frac{\eta_0^{p-1} \partial^p}{\partial \eta'^p} \quad Q_n(\eta') X_n(\eta', c^{(p+1)}) \right\}_{\eta'=\eta_0} .$$

Similarly the outside potential of a surface charge

$$\rho h_2 \sum_{0}^{\infty} c_n P_n$$

on a spheroid η_0 is

$$v^{>}(\xi, \eta) = 4\pi \rho k^2 \sum_{n=0}^{\infty} P_n(\xi) \cdot Q_n(\eta) P_n(\eta_0) X_n(\eta_0, c) ,$$

and the outside potential of a finite distortion is

$$v^{>}_{\text{dist}}(\eta, \xi) = 4\pi \rho k^2 \eta_0^2 \sum_{p=0}^{\infty} \frac{1}{(p+1)!} \sum_{n=0}^{\infty} P_n(\xi) \cdot U_{np}(\eta_0) \cdot \eta_0 Q_n(\eta),$$

where

$$U_{np}(\eta_0) = \left\{ \frac{\eta_0^{p-2} \partial^p}{\partial \eta'^p} \quad P_n(\eta') X_n(\eta', c^{(p+1)}) \right\}_{\eta'=\eta_0} .$$

Mudd's method gives the potential both inside and outside the distortion, but as one crosses into the distortion there is a discontinuity in the second and higher derivatives of the potential, so that the formulae derived above do not apply for points within the distortion. In order to overcome this limitation we make use of the fact that if, instead of considering the distortion by itself, we consider it simultaneously with the spheroid, then there is no discontinuity in any derivative of the total potential (i.e., that due to spheroid plus distortion) when crossing from the inside of the spheroid into the distortion in regions where the new surface is outside the old, and similarly there is no discontinuity when crossing from outside the

spheroid into the distortion in regions where the new surface is inside the old. Hence the appropriate expression for the total potential may be carried over into the region of the distortion and then, by subtraction of the potential due to the spheroid (known everywhere), the potential inside the distortion may be obtained.

Consider in particular the case when the new surface is entirely outside the spheroid. Then we have

$$\begin{aligned} v_{dist}\,(\text{at points within distortion}) &= v_{dist}(\text{dist}) \\ &= v_{\text{new shape}}(\text{dist}) - v_{sph}(\text{dist}) \\ &= v_{sph\,+\,dist}(\text{dist}) - v_{sph}(\text{dist}) \\ &= v^{<}_{sph\,+\,dist}(\text{dist}) - v^{>}_{sph}(\text{dist}) . \end{aligned}$$

The first term in the last line means that the expression for the total potential appropriate to the inside of the spheroid may be used also in the region of the distortion, since there is no discontinuity across the surface of the spheroid. Finally we obtain

$$v_{dist}\,(\text{dist}) = v^{<}_{sph}(\text{dist}) + v^{<}_{dist}\,(\text{dist}) - v^{>}_{sph}\,(\text{dist}) .$$

In this way we have expressed the unknown $v_{dist}\,(\text{dist})$ in terms of $v^{<}_{dist}$, which is available. Using the above relation, we find

$$\begin{aligned} E_{dist} + E_{int} &= \rho \int_{dist} \left[\tfrac{1}{2} \left(v^{<}_{sph} + v^{<}_{dist} - v^{>}_{sph} \right) + v^{>}_{sph} \right] \\ &= \rho \int_{dist} \left[\tfrac{1}{2} \left(v^{<}_{sph} + v^{>}_{sph} \right) + \tfrac{1}{2}\, v^{<}_{dist} \right] . \end{aligned} \tag{8}$$

The inside and outside potentials due to a uniformly charged spheroid are obtained by an integration over contributions due to spheroidal shells of charge η' to $\eta' + d\eta'$. The result can be written

$$v^{<}_{sph}\,(\eta, \xi) = 4\pi\rho k^2 \sum_{n=0}^{2} P_n(\xi) \cdot L_n\,(\eta_0, \eta) ,$$

$$v^{>}_{sph}\,(\eta, \xi) = 4\pi\rho k^2 \sum_{n=0}^{2} P_n(\xi) \cdot K_n\,(\eta_0, \eta) ,$$

where

$$L_n = Q_n(\eta) \int_1^{\eta} P_n(\eta') X_n(\eta')\, d\eta' + P_n(\eta) \int_{\eta}^{\eta_0} Q_n(\eta') X_n(\eta')\, d\eta' ,$$

$$K_n = Q_n(\eta) \int_1^{\eta_0} P_n(\eta') X_n(\eta') d\eta' ,$$

with

$$X_0(\eta') = \eta'^2 - \frac{1}{3} ,$$

$$X_2(\eta') = -\frac{2}{3} ,$$

$$X_n(\eta') = 0 \text{ for } n > 2.$$

Evaluation of the integrals gives

$$L_0 = [\frac{1}{3}(\eta_0^3 - \eta_0) Q_0(\eta_0) + \frac{1}{6}\eta_0^2] - \frac{1}{6}\eta^2 ,$$

$$L_2 = [\frac{1}{6}(\eta_0^3 - \eta_0) Q_0(\eta_0) - \frac{1}{6}\eta_0^2] + [-\frac{1}{3} + \frac{1}{2}\eta_0^2 - \frac{1}{2}(\eta_0^3 - \eta_0) Q_0(\eta_0)]\eta^2 ,$$

$$L_{n\geq 2} = 0 ,$$

$$K_0 = \frac{1}{3}(\eta_0^3 - \eta_0) Q_0(\eta) ,$$

$$K_2 = -\frac{1}{3}(\eta_0^3 - \eta_0) Q_2(\eta) ,$$

$$K_{n\geq 2} = 0.$$

Note also the expression

$$\frac{1}{2}(v_{sph}^{<} + v_{sph}^{>}) = 4\pi\rho k^2 \cdot \sum_{n=0}^{2} P_n(\xi) \cdot G_n(\eta_0, \eta) ,$$

where

$$G_n = \frac{1}{2}(K_n + L_n) .$$

The electrostatic energy of the spheroid may be obtained by an integral over $v_{sph}^{<}$, with the result

$$E_{sph} = E_c^{(0)} \cdot (\eta_0^3 - \eta_0)^{1/3} Q_0(\eta_0) , \quad E_c^{(0)} = \frac{16}{15}\pi^2\rho^2 R_0^5 .$$

With $\frac{1}{2}(v^{<}_{sph} + v^{>}_{sph})$ and $\frac{1}{2}\, v^{<}_{dist}$ available we now substitute in Eq. (8) and carry out the final integration over the distortion, using for the second time the trick of expanding the integrand in a Taylor series, interchanging the order of integrations and differentiations, and integrating term by term (after having first replaced

$$\sum_0^2 (\eta^2 - \xi^2)\, P_n\, G_n \quad \text{by} \quad \sum_0^4 P_n\, X_n\, (\eta, G) \text{ according to}$$

Eq. (7a)):

$$\rho \int_{dist} \frac{1}{2}\, (v^{<}_{sph} + v^{>}_{sph}) =$$

$$= \rho \int_{-1}^{1} \int_{0}^{2\pi} d\xi d\phi \int_{\eta_0}^{\eta_0+\Delta} d\eta h_1 h_2 h_3 \cdot 4\pi\rho k^2 \sum_0^2 P_n(\xi)\, G_n(\eta_0, \eta) =$$

$$= 8\pi^2\rho^2 k^5 \int_{-1}^{1} d\xi \int_{\eta_0}^{\eta_0+\Delta} \sum_0^4 P_n(\xi)\, X_n\, (\eta, G) =$$

$$= 8\pi^2\rho^2 k^5 \sum_{n=0}^{4} \int_{-1}^{1} d\xi\, P_n(\xi) \sum_{p=0}^{\infty} \frac{(\delta)^{p+1}}{(p+1)!} \left\{ \frac{\eta_0^{\,p+1} \partial^p X_n(\eta, G)}{\partial \eta^p} \right\}_{\eta=\eta_0} =$$

$$= 8\pi^2\rho^2 k^5 \eta_0^{\,5} \sum_{p=0}^{\infty} \frac{1}{(p+1)!} \sum_{n=0}^{4} \frac{2}{2n+1}\, c_n^{(p+1)} \left\{ \frac{\eta_0^{\,p-4} \partial^p X_p(\eta, G)}{\partial \eta^p} \right\}_{\eta=\eta_0}.$$

Proceeding similarly, we obtain

$$\rho \int_{dist} \frac{1}{2}\, v^{<}_{dist} = \frac{1}{2}\, \rho \int_{-1}^{1} \int_{0}^{2\pi} d\xi d\phi \int_{\eta_0}^{\eta_0+\Delta} d\eta h_1 h_2 h_3 \cdot 4\pi\rho k^2 \eta_0^{\,2} \cdot$$

$$\cdot \sum_{p=0}^{\infty} \frac{1}{(p+1)!} \sum_{n=0}^{\infty} P_n(\xi) \cdot W_{np}(\eta_0)\, P_n(\eta) =$$

$$= 2\pi\rho^2 k^5 \eta_0^5 \int_{-1}^{1}\int_{0}^{2\pi} d\xi\, d\phi \sum_{p,q=0}^{\infty} \frac{1}{(p+1)!\,(q+1)!} \sum_{n=0}^{\infty} P_n(\xi) \cdot$$

$$\cdot \sum_{m=0}^{\infty} P_m(\xi) \cdot W_{np}(\eta_0) \left\{ \frac{\eta_0^{q-2}\partial^q}{\partial \eta^q} X_n(\eta, c^{(q+1)})\, P_n(\eta) \right\}_{\eta=\eta_0}$$

$$= 4\pi^2 \rho^2 k^5 \eta_0^5 \sum_{p=0}^{\infty} \sum_{q=0}^{\infty} \frac{1}{(p+1)!\,(q+1)!} \sum_{n=0}^{\infty} \frac{2}{2n+1} W_{np}(\eta_0) U_{nq}(\eta_0).$$

Expressing all energies in units of the electrostatic energy of the sphere, $E_c^{(0)}$, and using $k = R_0/(\eta_0^3 - \eta_0)^{1/3}$, we obtain the final result

$$B_c = \frac{E_c}{E_c^{(0)}} = (e^{-3} - e^{-1})^{1/3} Q_0(e^{-1}) +$$

$$+ 15\,(1-e^2)^{-5/3} \cdot \sum_{p=0}^{\infty} \frac{1}{(p+1)!} \sum_{n=0}^{4} \frac{1}{2n+1} c_n^{(p+1)} T_{np}(e^{-1}) +$$

$$+ \frac{15}{2}\,(1-e^2)^{-5/3} \sum_{p,q=0}^{\infty} \frac{1}{(p+1)!\,(q+1)!} \sum_{n=0}^{\infty} \frac{1}{2n+1} Z_{npq}(e^{-1})$$

where

$$T_{np}(\eta_0) = \left\{ \eta_0^{p-4} \frac{\partial^p X_n(\eta, G)}{\partial \eta^p} \right\}_{\eta=\eta_0},$$

$$Z_{npq}(\eta_0) = \left\{ \eta_0^{p-1} \frac{\partial^p}{\partial \eta^p} X_n(\eta, c^{(p+1)})\, Q_n(\eta) \right\}_{\eta=\eta_0}$$

$$\cdot \left\{ \eta_0^{q-2} \frac{\partial^q}{\partial \eta^q} X_n(\eta, c^{(q+1)})\, P_n(\eta) \right\}_{\eta=\eta_0}.$$

The above formula, which, when worked out, gives a power expansion in the coefficients a_0, a_1, a_2 ... , was obtained by use of Eq. (8), derived on the assumption that the distortion is entirely outside the spheroid. This means that, in the first place, the formula

is justified only in a part of the deformation space of the a_n's, namely the part where a_0 satisfies a certain inequality $a_0 > f(a_1, a_2, \ldots)$, ensuring the required condition. If the total electrostatic energy, considered as a function of a_0, has no singularities in the neighborhood in question, the same power expansion holds also for other small distortions, even when the new surface does intersect the old. It has been verified explicitly that assuming the new surface to be entirely inside the old and using the resulting formula,

$$E_{dist} + E_{int} = \rho \int_{dist} [\tfrac{1}{2}(v_{sph}^{<} + v_{sph}^{>}) + \tfrac{1}{2} v_{dist}^{>}] ,$$

leads to the same power expansion for E_c as before, but the validity of the formula has not been verified explicitly in the case in which the old and new surfaces intersect. The problem of the range of validity of the above expansions requires further analysis.

4. Expansions About a Sphere

By taking the limit $\eta_0 \to \infty$ we obtain expansions about the spherical shape:

$$\frac{\delta V}{V_0} = 3a_0 + 3 \sum_{n=0}^{\infty} \frac{a_n^2}{2n+1} + \frac{1}{2} \sum_{p,q,r=0}^{\infty} (pqr)\, a_p a_q a_r$$

$$V\bar{z} = \frac{4}{3}\pi R_0^4 \left\{ c_1^{(1)} + \frac{3}{2} c_1^{(2)} + c_1^{(3)} + \frac{1}{4} c_1^{(4)} \right\} . \qquad (9)$$

In the case of the surface area the expression

$$F_{n,s} = \left\{ \frac{\partial^{n+s}}{\partial x^n \partial z^s} F(x,z) \right\}_{\substack{z=1 \\ z=B^2}}$$

becomes

$$F_{n,s} = \left\{ \frac{\partial^{n+s}}{\partial x^n \partial z^s} x\sqrt{x^2 - 1 + z} \right\}_{\substack{x=1 \\ z=1}} =$$

$$= \frac{1}{2} \cdot \frac{-1}{2} \cdot \frac{-3}{2} \ldots \text{(s factors)} \cdot (2-2s)(2-2s-1) \ldots$$

$$\ldots \text{(n factors)}.$$

Hence we have

$$B_s = \sum_{n=0}^{\infty} \sum_{s=0}^{\infty} \frac{\frac{1}{2} \cdot \frac{-1}{2} \cdot \frac{-3}{2} \cdots \text{(s factors)} \cdot (2-2s)(2-2s-1) \cdots \text{(n factors)}}{n!\ s!}$$

$$\sum_{i=0}^{\infty} \frac{c_i(n)\, d_i(s)}{2i+1} \quad .$$

In reducing the formulae for the electrostatic energy we make use of the following limiting expressions for $\eta \to \infty$:

$$P_n(\eta) \to \frac{(2n)!}{2^n (n!)^2}\ \eta^n \ ,$$

$$Q_n(\eta) \to \frac{2^n (n!)^2}{(2n+1)!}\ \eta^{-n-1} \ ,$$

which lead to

$$G_0 \to \frac{1}{6}\,\eta_0{}^3 \eta^{-1} + \frac{1}{4}\,\eta_0{}^2 - \frac{1}{12}\,\eta^2 \ ,$$

$$G_n / G_0 \to 0 \text{ for } n > 0.$$

We find further

$$X_n(\eta, c^{(q+1)}) \to \eta^2 c^{(q+1)},$$

$$X_n(\eta, G) \to \eta^2 G_n \ .$$

Hence only the term with n = 0 survives in the sum over $T_{np}(\eta_0)$:

$$T_{0p}(\eta_0) \to \left\{ \eta_0{}^{p-4}\ \frac{\partial^p}{\partial \eta^p} \left(\frac{1}{6}\,\eta_0{}^3 \eta + \frac{1}{4}\,\eta_0{}^2 \eta^2 - \frac{1}{12}\eta^4 \right) \right\}_{\eta=\eta_0}$$

$$= \frac{1}{3}, \quad \frac{1}{3}, \quad \frac{-1}{2}, \quad -2, \quad -2 \text{ for } p = 0,\ 1,\ 2,\ 3,\ 4 \text{ respectively,}$$

$$= 0 \text{ for } p > 4.$$

The expression $Z_{npq}(\eta_0)$ tends to

$$\left\{\eta_0^{p-1}\,\frac{\partial^p}{\partial\eta^p}\,\eta^2\,c_n^{(p+1)}\,\frac{2^n(n!)^2}{(2n+1)!}\,\eta^{-n-1}\right\}_{\eta=\eta_0} \times$$

$$\times\left\{\eta_0^{q-2}\,\frac{\partial^q}{\partial\eta^q}\,\eta^2\,c_n^{(q+1)}\,\frac{(2n)!}{2^n(n!)^2}\,\eta^n\right\}_{\eta=\eta_0}$$

$$= \frac{c_n^{(p+1)}c_n^{(q+1)}}{2n+1}\left\{\frac{\partial^q}{\partial x^q}\,x^{n+2}\,\frac{\partial^p}{\partial y^p}\,y^{-n+1}\right\}_{x=y=1}.$$

Hence the formula for the electrostatic energy reduces to

$$\frac{E_c}{E_c^{(0)}} = 1 + 5c_0^{(1)} + \frac{5}{2}\,c_0^{(2)} - \frac{5}{4}\,c_0^{(3)} - \frac{5}{4}\,c_0^{(4)} - \frac{1}{4}\,c_0^{(5)} +$$

$$+ \frac{15}{2}\sum_{p,\,q=0}^{\infty}\frac{1}{(p+1)!\,(q+1)!}\sum_{n=0}^{\infty}\frac{c_n^{(p+1)}c_n^{(q+1)}}{(2n+1)^2} \times$$

$$\times (n+2)(n+1)\ldots(q \text{ factors})\cdot(-n+1)(-n)\cdots(p \text{ factors}).$$

So far the most extensive applications of the general formulae have been made to the study of the energy in the neighborhood of the spherical shape. We shall present the results of an expansion in which the distortion was specified by

$$R(\theta) = \lambda^{-1} R_0\left[1 + \sum_{n=1}^{5} a_n P_n(\cos\theta)\right] = \lambda^{-1} R_0(1+\delta),$$

where n = 0 is not included in the sum, and λ is a scale factor providing an alternative way of preserving the volume. It is given by $\lambda^3 = (V_0 + \delta V)/V_0$, where $V_0 + \delta V$ is the volume of the shape $R_0(1+\delta)$.

The energies were worked out to the sixth order in a small quantity u, the different coefficients a_n being regarded as of different

orders in u, according to the following scheme: a_1 of order u^2, a_2 and a_3 of order u, a_4 and a_5 of order u^2. This choice was designed so that terms contributing to an expansion of the conventional threshold energy to sixth order in the quantity (1-x) would be retained automatically. Terms involving a_6, which are also required for this purpose, were included later, as well as certain terms in a_7. In this connection we should like to note that our criticism in Ref. 2 of Nossoff's statement that a_{2n} is of order $(1-x)^n$ was incorrect.

5. The Coefficients $c_n^{(p)}$ and $d_n^{(p)}$.

The coefficients $c_n^{(p)}$, specifying the expansion of the pth power of δ, would occur in any problem where distorted spheres or spheroids were used, and they are given, therefore, as fully as they are available. The calculations were made with six decimals, all of which are reproduced, although rounding off errors affect the last digit. The selection of the terms retained is based, broadly speaking, on the scheme explained above. The coefficients are:

For p = 0

$c_0 = 1$, all other c's equal to zero.

For p = 1

$c_0 = 0$, $c_1 = a_1$, $c_2 = a_2$, $c_3 = a_3$, $c_4 = a_4$, $c_5 = a_5$.

For p = 2

$$c_0 = 0.333333a_1^2 + 0.200000a_2^2 + 0.142857a_3^2 + 0.111111a_4^2 + \\ + 0.090909a_5^2.$$

$$c_1 = 0.800000a_1a_2 + 0.514286a_2a_3 + 0.380952a_3a_4 + 0.303030a_4a_5.$$

$$c_2 = 0.666667a_1^2 + 0.857143a_1a_3 + 0.285714a_2^2 + 0.571429a_2a_4 + \\ + 0.190476a_3^2 + 0.432901a_3a_5 + 0.144300a_4^2 + 0.116550a_5^2.$$

$$c_3 = 1.200000a_1a_2 + 0.888889a_1a_4 + 0.533334a_2a_3 + 0.606061a_2a_5 + \\ + 0.363637a_3a_4 + 0.279720a_4a_5.$$

$$c_4 = 1.142857a_1a_3 + 0.909091a_1a_5 + 0.514286a_2^2 + 0.519481a_2a_4 + \\ + 0.233766a_3^2 + 0.359640a_3a_5 + 0.161838a_4^2 + 0.125874a_5^2.$$

$$c_5 = 1.111111a_1a_4 + 0.952381a_2a_3 + 0.512820a_2a_5 + 0.439560a_3a_4 +$$
$$+ 0.307692a_4a_5.$$

$$c_6 = 1.090909a_1a_5 + 0.909091a_2a_4 + 0.432901a_3^2 + 0.424242a_3a_5 +$$
$$+ 0.202020a_4^2 + 0.142602a_5^2.$$

$$c_7 = 0.881120a_2a_5 + 0.815852a_3a_4 .$$

$$c_8 = 0.783217a_3a_5.$$

For p = 3

$$c_0 = 0.400000a_1^2a_2 + 0.514286a_1a_2a_3 + 0.380952a_1a_3a_4 + 0.303030a_1a_4a_5 +$$
$$+ 0.057143a_2^3 + 0.171429a_2^2a_4 + 0.114286a_2a_3^2 + 0.259740a_2a_3a_5 +$$
$$+ 0.086580a_2a_4^2 + 0.069930a_2a_5^2 + 0.077922a_3^2a_4 + 0.119880\ a_3a_4a_5 +$$
$$+ 0.017982a_4^3 + 0.041958a_4a_5^2.$$

$$c_1 = 0.942857a_1a_2^2 + 0.657143a_1a_3^2 + 0.514286a_2^2a_3 + 0.737663a_2a_3a_4 +$$
$$+0.233766a_2^2a_5 + 0.093506a_3^3 + 0.269730a_3^2a_5 + 0.685714a_1a_2a_4 +$$
$$+0.506493a_1a_4^2.$$

$$c_2 = 1.571429a_1^2a_2 + 1.714286a_1a_2a_3 + 1.229438a_1a_3a_4 + 0.779221a_1a_2a_5 +$$
$$+ 0.428571a_2^3 + 0.792208a_2a_3^2 + 0.595738a_2a_4^2 + 0.480520a_2a_5^2 +$$
$$+ 0.467533a_2^2a_4 + 0.679321a_2a_3a_5 + 0.491509a_3^2a_4 +$$
$$+ 0.749251a_3a_4a_5.$$

$$c_3 = 1.533333a_1^2a_3 + 1.200000a_1a_2^2 + 1.721213a_1a_2a_4 + 0.654546a_1a_3^2 +$$
$$+ 1.258742a_1a_3a_5 + 1.109092\ a_2^2a_3 + 1.376224a_2a_3a_4 +$$

$$+ 1.048951a_2a_4a_5 + 0.475524a_2^2a_5 + 0.337063a_3^3 + 0.419580a_3^2a_5 +$$

$$+ 0.678322a_3a_4^2 + 0.534348a_3a_5^2.$$

$$c_4 = 2.212988a_1a_2a_3 + 0.280520a_2^3 + 1.072328a_2^2a_4 + 0.884716a_2a_3^2 +$$

$$+ 1.348652a_2a_3a_5 + 0.872128a_3^2a_4.$$

$$c_5 = 0.857143a_1a_2^2 + 0.989011a_1a_3^2 + 0.747253a_2^2a_3 + 1.057143a_2^2a_5 +$$

$$+ 1.648352a_2a_3a_4 + 0.219780a_3^3 + 0.839689a_3^2a_5.$$

$$c_6 = 1.558442a_1a_2a_3 + 0.233767a_2^3 + 0.701299a_2^2a_4 + 0.649351a_2a_3^2 +$$

$$+ 1.588387a_2a_3a_5 + 0.595875a_3^2a_4.$$

$$c_7 = 0.629372a_2^2a_3 + 0.185109a_3^3.$$

$$c_8 = 0.559441a_2a_3^2.$$

For p = 4

$$c_0 = 0.628572a_1^2a_2^2 + 0.438095a_1^2a_3^2 + 0.685714a_1a_2^2a_3 +$$

$$+ 0.983550a_1a_2a_3a_4 + 0.311688a_1a_2^2a_5 + 0.124675a_1a_3^3 +$$

$$+ 0.359640a_1a_3^2a_5 + 0.085714a_2^4 + 0.316883a_2^2a_3^2 +$$

$$+ 0.238295a_2^2a_4^2 + 0.192208a_2^2a_5^2 + 0.124676a_2^3a_4 +$$

$$+ 0.271728a_2^2a_3a_5 + 0.393207a_2a_3^2a_4 + 0.599401a_2a_3a_4a_5 +$$

$$+ 0.048152a_3^4 + 0.079920a_3^3a_5 + 0.193806a_3^2a_4^2 + 0.152671a_3^2a_5^2.$$

$$c_1 = 0.654546a_2^3a_3 + 0.496304a_2a_3^3 + 0.914285a_1a_2^3 + 1.433767a_1a_2^2a_4.$$

$$c_2 = 3.272729a_1a_2^2a_3 + 0.827173a_1a_3^3 + 0.259741a_2^4 + 0.815186a_2^3a_4 +$$

$$+ 1.186814a_2^2a_3^2 + 1.678322a_2^2a_3a_5 + 1.870131a_2a_3^2a_4 +$$

$$+ 0.151848a_3^4 + 0.503026a_3^3a_5.$$

$$c_3 = 1.527273a_1a_2^3 + 3.474128a_1a_2a_3^2 + 1.107693a_2^3a_3 + 2.618184a_2^2a_3a_4 +$$
$$+ 0.783217a_2^3a_5 + 0.850350a_2a_3^3 + 2.112711a_2a_3^2a_5 + 0.675278a_3^3a_4.$$

$$c_4 = 0.366833a_2^4 + 1.683118a_2^2a_3^2 + 0.217053a_3^4.$$

$$c_5 = 1.230770a_2^3a_3 + 1.106658a_2a_3^3.$$

$$c_6 = 0.187013a_2^4 + 1.503439a_2^2a_3^2 + 0.225795a_3^4.$$

For p = 5

$$c_0 = 1.090910a_1a_2^3a_3 + 0.827173a_1a_2a_3^3 + 0.051948a_2^5 + 0.203796a_2^4a_4 +$$
$$+ 0.395605a_2^3a_3^2 + 0.559441a_2^3a_3a_5 + 0.935065a_2^2a_3^2a_4 +$$
$$+ 0.151848a_2a_3^4 + 0.503026a_2a_3^3a_5 + 0.120585a_3^4a_4.$$

$c_1 = 0$ to the required order in u.

$$c_2 = 0.264735a_2^5 + 1.894773a_2^3a_3^2 + 0.767762a_2a_3^4.$$

$$c_3 = 1.326341a_2^4a_3 + 2.149734a_2^2a_3^3 + 0.180742a_3^5.$$

The coefficients $d_n^{(p)}$ specifying the expansion of the pth power of $(1-\xi^2)(d\delta/d\xi)^2$ are given below, again with a selection of terms based on the "sixth-order" expansion discussed previously.

For p = 0

$d_0 = 1$, all other d_n's equal to zero.

For p = 1

$$d_0 = 0.666667a_1^2 + 1.200000a_2^2 + 1.714286a_3^2 + 2.222222a_4^2 +$$
$$+ 2.727273a_5^2.$$

$$d_1 = 2.400000a_1a_2 + 4.114285a_2a_3 + 5.714285a_3a_4 + 7.272727a_4a_5.$$

$$d_2 = 3.428572a_1a_3 + 0.857142a_2^2 + 5.714285a_2a_4 + 1.714286a_3^2 +$$
$$+ 7.792208a_3a_5 - 0.666667a_1^2 + 2.453101a_4^2 + 3.146853a_5^2.$$

$$d_3 = 4.444446a_1a_4 + 1.600001a_2a_3 + 7.272729a_2a_5 + 3.636363a_3a_4 -$$
$$- 2.400000a_1a_2 + 5.314686a_4a_5.$$

$$d_4 = 5.454547a_1a_5 + 1.558441a_2a_4 + 0.467532a_3^2 + 3.956044a_3a_5 -$$
$$- 3.428572a_1a_3 + 1.618382a_4^2 - 2.057142a_2^2 + 2.517482a_5^2.$$

$$d_5 = 1.538462a_2a_5 + 0.439560a_3a_4 - 4.444445a_1a_4 + 3.076922a_4a_5 -$$
$$- 5.714285a_2a_3.$$

$$d_6 = -5.454549a_1a_5 - 0.202020a_4^2 - 7.272728a_2a_4 + 1.283423a_5^2 -$$
$$- 3.896105a_3^2.$$

$$d_7 = - 8.811190a_2a_5 - 9.790209a_3a_4.$$

$$d_8 = - 11.748256a_3a_5.$$

For p = 2

$$d_0 = 4.114285a_1^2a_2^2 + 5.485716a_1^2a_3^2 + 2.057142a_2^4 + 13.464933a_2^2a_3^2 +$$
$$+ 16.303695a_2^2a_4^2 + 19.420581a_2^2a_5^2 + 4.718483a_3^4 +$$
$$+ 28.771222a_3^2a_4^2 + 33.002302a_3^2a_5^2 + 8.228568a_1a_2^2a_3 +$$
$$+ 19.948055a_1a_2a_3a_4 + 25.318681a_2a_3^2a_4 + 57.542450a_2a_3a_4a_5 +$$
$$+ 1.994806a_1a_3^3 + 11.508496a_1a_3^2a_5 + 1.246751a_2^3a_4 +$$
$$+ 2.589410a_2^2a_3a_5 + 5.754246a_3^3a_5 - 7.480518a_1a_2^2a_5.$$

$$d_1 = 15.709085a_2^3a_3 + 26.239368a_2a_3^3 .$$

$$d_2 = 18.701302a_1a_2^2a_3 + 1.870127a_2^4 + 14.865133a_2^3a_4 + 25.894098a_2^2a_3^2 +$$
$$+ 38.841177a_2^2a_3a_5 + 16.879128a_1a_3^3 + 92.067936a_2a_3^2a_4 +$$
$$+8.055944a_3^4 + 47.049420a_3^3a_5.$$

$$d_3 = 0.402796a_2^3a_3 + 22.153850a_2^3a_5 + 32.223771a_2^2a_3a_4 - 6.981816a_1a_2^3 +$$
$$+ 12.889508a_2a_3^3 + 75.346808a_2a_3^2a_5 + 29.696412a_3^3a_4 -$$
$$- 1.61187a_1a_2a_3^2.$$

$$d_4 = - 18.643756a_2^2a_3^2 - 4.790408a_2^4 + 0.426489a_3^4.$$

$$d_5 = -22.153836a_2^3a_3 - 32.020693a_2a_3^2.$$

$$d_6 = -35.642471a_2^2a_3^2 - 14.822088a_3^4 - 0.748051a_2^4.$$

For p = 3

$$d_0 = 3.884112a_2^6 + 62.145826a_2^4a_3^2 + 104.185712a_2^2a_3^4 +$$
$$+ 15.315209a_3^6.$$

6. The Electrostatic and Surface Energies

The electrostatic and surface energies as well as the scale factor λ^3 were first calculated for the shape $R_0(1+\delta)$. The energies of the volume-preserving shape $\lambda^{-1}R_0(1+\delta)$ were then found by multiplying by the scaling factors λ^{-5} and λ^{-2}, respectively.

The result was

$$B_c = E_c/E_c^{(0)} =$$
$$= 1.000000 - 0.200000a_2^2 - 0.204081a_3^2 - 0.185186a_4^2 -$$
$$-0.165289a_5^2 + 0.133333a_1^2a_2 - 0.195919a_1a_2a_3 - 0.272108a_1a_3a_4 -$$
$$-0.275483a_1a_4a_5 - 0.038095\,a_2^3 - 0.171430a_2^2a_4 - 0.125171a_2a_3^2 -$$

$$-0.335075a_2a_3a_5 - 0.115440a_2a_4^2 - 0.103835a_2a_5^2 - 0.111317a_3^2a_4 -$$

$$-0.194610\,a_3a_4a_5 - 0.029970a_4^3 - 0.076287a_4a_5^2 + 0.601358a_1^2a_2^2 +$$

$$+ 0.397278a_1^2a_3^2 + 0.440816a_1a_2^2a_3 + 0.418193a_1a_2a_3a_4 -$$

$$- 0.046551a_1a_2^2a_5 + 0.035622a_1a_3^3 + 0.082156a_1a_3^2a_5 + 0.208163a_2^4 +$$

$$+ 0.534345a_2^2a_3^2 + 0.383651a_2^2a_4^2 + 0.305995a_2^2a_5^2 + 0.032652a_2^3a_4 +$$

$$+ 0.030342a_2^2a_3a_5 + 0.311275a_2a_3^2a_4 + 0.374710a_2a_3a_4a_5 +$$

$$+ 0.166812a_3^4 + 0.036620a_3^3a_5 + 0.419291a_3^2a_4^2 + 0.318544a_3^2a_5^2 +$$

$$+ 0.445944a_1a_2^3a_3 + 0.397171a_1a_2a_3^3 + 0.046508a_2^5 + 0.208406a_2^4a_4 +$$

$$+ 0.271293a_2^3a_3^2 + 0.451810a_2^3a_3a_5 + 0.554265a_2^2a_3^2a_4 +$$

$$+0.147106a_2a_3^4 + 0.425058a_2a_3^3a_5 + 0.129865a_3^4a_4 - 0.182764a_2^6 -$$

$$- 0.827188a_2^4a_3^2 - 0.750764a_2^2a_3^4 - 0.197173a_3^6 + \ldots$$

(10)

$$B_s = E_s/E_s^{(0)} =$$

$$= 1.000000 + 0.400000a_2^2 + 0.714286a_3^2 + 1.000000a_4^2 + 1.272727a_5^2 -$$

$$- 0.342858a_1a_2a_3 - 0.038095a_2^3 - 0.114286a_2^2a_4 - 0.076191a_2a_3^2 -$$

$$- 0.173160a_2a_3a_5 - 0.051948a_3^2a_4 - 0.266667a_1^2a_2 - 0.253968a_1a_3a_4 -$$

$$- 0.202020a_1a_4a_5 - 0.057720a_2a_4^2 - 0.046620a_2a_5^2 - 0.079920a_3a_4a_5 -$$

$$-0.11988a_4^3 - 0.027972a_4a_5^2 - 0.647619a_1^2a_2^2 - 1.066668a_1^2a_3^2 -$$

$$- 0.377143a_2^4 - 2.025974a_2^2a_3^2 - 2.482406a_2^2a_4^2 - 2.973027a_2^2a_5^2 -$$

$$- 0.773483a_3^4 - 4.009101a_3^2a_4^2 - 4.592820a_3^2a_5^2 - 1.028571a_1a_2^2a_3 -$$

$$- 2.493507a_1a_2a_3a_4 - 3.164835a_2a_3^2a_4 - 7.192806a_2a_3a_4a_5 -$$

$$- 0.249351a_1a_3^3 - 1.438562a_1a_3^2a_5 - 0.155844a_2^3a_4 - 0.323676a_2^2a_3a_5 -$$

$$- 0.719281a_3^3a_5 + 0.935065a_1a_2^2a_5 + 2.063377a_1a_2^3a_3 +$$

$$+ 2.875068a_1a_2a_3^3 + 0.101126a_2^5 + 0.633047a_2^4a_4 + 1.313444a_2^3a_3^2 +$$

$$+ 2.264404\, a_2^3a_3a_5 + 5.214100a_2^2a_3^2a_4 + 0.841368a_2a_3^4 +$$

$$+ 4.266212a_2a_3^3a_5 + 1.057591a_3^4a_4 + 0.309053a_2^6 + 3.414835a_2^4a_3^2 +$$

$$+ 5.424081a_2^2a_3^4 + 1.001962a_3^6 + \ldots \qquad (11)$$

The center of mass of the shape undergoing the distortion may be held fixed at the origin by making a_1 a suitable function of the other a_n's, in such a way that the expression for $\bar{z}$, given by Eq. (9), is equal to zero. Working within the "sixth-order" approximation, the following expression for a_1 was used:

$$a_1 = - 0.771429a_2a_3 + 0.411429a_2^2a_3 - 0.093506a_3^3 - 0.571428a_3a_4 +$$

$$+ 0.069996a_2^3a_3 + 0.495071a_2a_3^3 - 0.051950a_2a_3a_4 - 0.454545a_4a_5 -$$

$$- 0.233766a_2^2a_5 - 0.269730a_3^2a_5 + \ldots$$

Substitution of this expression in Eqs. (10) and (11) resulted in the following formulae:

$$B_c =$$

$$= 1.000000 - 0.200000a_2^2 - 0.204081a_3^2 - 0.185186a_4^2 - 0.165289a_5^2 -$$

$$- 0.038095a_2^3 - 0.171430a_2^2a_4 - 0.125171a_2a_3^2 - 0.335075a_2a_3a_5 -$$

$$- 0.115440a_2a_4^2 - 0.103835a_2a_5^2 - 0.111317a_3^2a_4 -$$

$$- 0.194610a_3a_4a_5 - 0.029970a_4^3 - 0.076287a_4a_5^2 + 0.208163a_2^4 +$$

$$+ 0.685483a_2^2a_3^2 + 0.383651a_2^2a_4^2 + 0.305995a_2^2a_5^2 +$$

$$+ 0.032652a_2^3a_4 + 0.030342a_2^2a_3a_5 + 0.633141a_2a_3^2a_4 +$$

$$+ 0.676280a_2a_3a_4a_5 + 0.166812a_3^4 + 0.036620a_3^3a_5 +$$

$$+ 0.574781a_3^2a_4^2 + 0.318544a_3^2a_5^2 + 0.046508a_2^5 + 0.208406a_2^4a_4 -$$

$$- 0.070025a_2^3a_3^2 + 0.533520a_2^3a_3a_5 - 0.004460a_2^2a_3^2a_4 +$$

$$+ 0.137946a_2a_3^4 + 0.414526a_2a_3^3a_5 + 0.134953a_3^4a_4 -$$

$$- 0.182764a_2^6 - 0.730318a_2^4a_3^2 - 0.925053a_2^2a_3^4 - 0.200504a_3^6 + \ldots$$

(12)

$$B_s =$$

$$= 1.000000 + 0.400000a_2^2 + 0.714286a_3^2 + 1.000000a_4^2 +$$

$$+ 1.272727a_5^2 - 0.038095a_2^3 - 0.114286a_2^2a_4 - 0.076191a_2a_3^2 -$$

$$- 0.173160a_2a_3a_5 - 0.057720a_2a_4^2 - 0.046620a_2a_5^2 - 0.051948a_3^2a_4 -$$

$$- 0.079920a_3a_4a_5 - 0.011988a_4^3 - 0.027972a_4a_5^2 - 0.377143a_2^4 -$$

$$- 1.761483a_2^2a_3^2 - 2.482406a_2^2a_4^2 - 2.973027a_2^2a_5^2 - 0.155844a_2^3a_4 -$$

$$- 0.323676a_2^2a_3a_5 - 2.772998a_2a_3^2a_4 - 6.881118a_2a_3a_4a_5 -$$

$$- 0.773483a_3^4 - 0.719281a_3^3a_5 - 3.863977a_3^2a_4^2 - 4.592820a_3^2a_5^2 +$$

$$+ 0.101126a_2^5 + 0.633047a_2^4a_4 + 1.807157a_2^3a_3^2 + 1.623216a_2^3a_3a_5 +$$

$$+ 7.403637a_2^2a_3^2a_4 + 1.065784a_2a_3^4 + 5.468440a_2a_3^3a_5 + 1.223825a_3^4a_4 +$$

$$+ 0.309053a_2^6 + 1.159778a_2^4a_3^2 + 2.356770a_2^2a_3^4 + 1.025278a_3^6 + \ldots$$

(13)

In comparing the coefficients of the terms up to fourth order in a with the explicit formula of Ref. 3, an error was found in Nossoff's formula for B_c in the term resulting from the condition of a fixed center

of mass (the term in $a_m a_{m+1} a_n a_{n+1}$, discussed in Ref. 2).

Nossoff's expression (Ref. 2)

$$\ldots + 45 \sum_{m,n=2}^{\infty} \frac{(4n-7)\ (n+1)\ \ (m+1)}{(2m+1)(2m+3)(2n+1)^2(2n+3)}\ a_m a_{m+1} a_n a_{n+1} + \ldots$$

should be replaced by

$$\ldots + 90 \sum_{m,n=2}^{\infty} \frac{m+1}{(2m+1)(2m+3)} \cdot \frac{(n+1)(4n^2-n-6)}{(2n+1)^2(2n+3)^2}\ a_m a_{m+1} a_n a_{n+1} + \ldots .$$

After this correction all the coefficients up to fourth order are consistent, as regards both B_c and B_s (except for rounding off errors in the last decimal).

Additional terms involving a_6 and a_7, considered as of order u^3, were evaluated directly by use of Nossoff's (corrected) formula. (The center of mass is therefore fixed, and a_1 does not appear). The result was

$$\begin{aligned} B_c = {} & \text{Eq. (12)} \\ & - 0.147928 a_6^2 - 0.306616 a_2 a_4 a_6 - 0.022131 a_2^3 a_6 - \\ & - 0.133333 a_7^2 - 0.155522 a_3^2 a_6 - 0.171483 a_3 a_5 a_6 - 0.279720 a_3 a_4 a_7 - \\ & - 0.277685 a_2 a_5 a_7 - 0.066478 a_2^2 a_3 a_7 - 0.003226 a_2 a_3^2 a_6 - 0.084465 a_2 a_7^2 - \\ & - 0.058923 a_4 a_7^2 + 0.185206 a_2^2 a_7^2 + \ldots \end{aligned} \tag{14}$$

$$\begin{aligned} B_s = {} & \text{Eq. (13)} \\ & + 1.538461 a_6^2 - 0.139860 a_2 a_4 a_6 + 0.503496 a_2^3 a_6 + \\ & + 1.800000 a_7^2 - 0.066600 a_3^2 a_6 - 0.065268 a_3 a_5 a_6 - 0.108780 a_3 a_4 a_7 - \\ & - 0.117482 a_2 a_5 a_7 + 2.013986 a_2^2 a_3 a_7 + 0.000000 a_2 a_3^2 a_6 - \\ & - 0.033786 a_2 a_7^2 - 0.019641 a_4 a_7^2 - 3.985256 a_2^2 a_7^2 + \ldots \end{aligned} \tag{15}$$

The above formulae, together with Nossoff's fourth-order expressions, provide a fairly comprehensive description of the energy of a slightly distorted drop possessing axial symmetry. Only a fraction of the information contained in them has been explored. In the following sections we present some of the results of applications that have been made.

7. Small Symmetric Distortions

Confining ourselves to symmetric distortions, we may write the total deformation energy in units of $E_s^{(0)}$, given by $(B_s-1) + 2x(B_c-1)$, as

$$\begin{aligned}\xi_{sym} = {} & (0.000000 + 0.400000u)a_2^2 + (-0.114285 + 0.076190u)a_2^3 + \\ & + (0.039183 - 0.416326u)a_2^4 + (-0.457144 + 0.342858u)a_2^2a_4 + \\ & + (0.629630 + 0.370370u)a_4^2 + (0.194142 - 0.093016u)a_2^5 + \\ & + (-0.090538 - 0.065306u)a_2^3a_4 + (-0.288600 + 0.230880u)a_2a_4^2 + \\ & + (-0.056475 + 0.365528u)a_2^6 + (1.049859 - 0.416812u)a_2^4a_4 + \\ & + (-1.715102 - 0.767304u)a_2^2a_4^2 + (-0.071928 + 0.059940u)a_4^3 + \\ & + (0.459233 + 0.044263u)a_2^3a_6 + (1.242604 + 0.295858u)a_6^2 + \\ & + (-0.753093 + 0.613233u)a_2a_4a_6 + \ldots \end{aligned} \tag{16}$$

Here u stands for 1-x.

The above function of a_2, a_4, and a_6 is stationary for several distinct sets of the three variables (in addition to $a_2 = a_4 = a_6 = 0$). For x values in the range 0.7 to 0.1, however, all but one of the sets occur at distortions so large that the expansion is not expected to be reliable, and it is not known whether any significance is to be attached to those saddle points.

The family of the conventional saddle-point shapes which includes the sphere for u = 0 may be studied by solving the system of equations

$$\frac{\partial \xi}{\partial a_2} = 0, \qquad \frac{\partial \xi}{\partial a_4} = 0, \qquad \frac{\partial \xi}{\partial a_6} = 0$$

in successive orders of u. The result is

$$\left.\begin{aligned} (a_2)_{sp} &= 2.333333u - 1.226170u^2 + 9.499768u^3 - 8.050944u^4 \ \ldots \\ (a_4)_{sp} &= 1.976474u^2 - 1.695026u^3 + 17.741912u^4 + \ldots \\ (a_6)_{sp} &= -0.949967u^3 + \ldots \ . \end{aligned}\right\} \quad (16a)$$

Substitution in Eq. (16) gives the expansion to order $(1-x)^6$ of the threshold energy,

$$\xi_{sp} = 0.725926u^3 - 0.330239u^4 + 1.920798u^5 - 0.212537u^6 + \ldots \quad (17)$$

No coefficient in this expression would be affected by the inclusion of further terms in the expansion of the deformation energy in powers of a_n.

Because of the cancellation of large terms there is a loss of accuracy, especially in the last term, which may amount to several units in the fourth decimal place in the coefficient of u^6.

The saddle-point shapes, as calculated in four orders of approximation for x = 0.7, are compared in Figs. 12(a), (b), (c), (d) with the shape calculated in Ref. 2. Figure 13 shows a comparison of the trends with x in the radius vectors of these shapes at angles of 0°, 40°, and 90°.

In Fig. 14 the sixth-order expansion for the threshold energy is compared with previous calculations.

The above results, which give the energy and location of the saddle point as a function of x, may be modified to yield the energy of a drop with a fixed x, distorted anywhere along the family of saddle-point shapes as specified, for example, by Eq. (16a), or by the shapes in Fig. 8 of Ref. 2. Let us label this sequence by a parameter t, equal to the value of 1-x at which the shape in question is a saddle-point shape (compare Ref. 4). Let the quantities (B_s-1) and (B_c-1), considered as functions of t, be denoted by f(t) and g(t), respectively. Then the deformation energy (always in units of $E_s^{(0)}$) of a drop carrying a charge corresponding to a value x (=1-u) and deformed to a shape specified by t is a function of u and t which we shall write as $\xi(u, t)$:

$$\xi\ (u, t) = f(t) + 2xg(t)$$

$$= f(t) + 2g(t) - 2ug(t).$$

Taking u = t corresponds to selecting a sequence of saddle-point configurations, whose energy

$$\xi(u, u) = f(u) + 2(1-u)g(u) \equiv F(u) \qquad (18)$$

is a function that gives the threshold for a given u, and to which an approximation is provided, for example, by Eq. (17).

As outlined in Ref. 2, the functions f and g may be derived from the key function F as follows. At the saddle point the energy is stationary with respect to all displacements, so that we have

$$\left(\frac{\partial \xi}{\partial t}\right)_{t = u} = 0\ ,$$

i.e.,

$$f'(u) + 2g'(u) - 2ug'(u) = 0.$$

On the other hand it follows from Eq. (18) that

$$F'(u) = f'(u) + 2g'(u) - 2g(u) - 2ug'(u)\ .$$

Combining these equations, we find

$$g(u) = -\ \tfrac{1}{2} F'(u)\ .$$

With g available, f follows from Eq. (18):

$$f(u) = F(u) + F'(u) - uF'(u)\ .$$

The relative electrostatic energy along the t-family of shapes is then found to be given by

$$B_c = 1+g(t) = 1-1.088889\ t^2 + 0.660478\ t^3 - 4.801995\ t^4 + 0.637611\ t^5 + \ldots\ ,$$

and the relative surface energy is

$$B_s = 1+f(t) = 1+2.177778\ t^2 - 2.772808\ t^3 + 10.594707\ t^4 - 8.958414\ t^5 +$$

$$+ 1.062685\ t^6 + \ldots\ .$$

The total deformation energy for any u, t can now be written entirely in terms of F and its derivative:

$$\xi(u, t) = F(t) + (u-t)F'(t)\ .$$

We verify that the derivative

$$\frac{\partial \xi(u, t)}{\partial t} = (u-t)F''(t)$$

vanishes for $u = t$.

The second derivative of the energy with respect to t is

$$\frac{\partial^2 \xi(u, t)}{\partial t^2} = - F''(t) + (u-t)F'''(t) .$$

For a saddle-point shape this becomes $-F''(u)$, where

$$F''(u) = 4.355556u - 3.962868u^2 + 38.415960u^3 - 6.376110u^4 + \ldots .$$

It follows that for an x value at which the threshold function F(u) is concave upwards, a t-type distortion away from the saddle point is towards decreasing energies, but when F(u) is convex, a t-type distortion is towards increasing energies. The former situation occurs when x is close to 1; the latter is exemplified, for example, in the limiting case of $x \ll 1$, discussed earlier. At an x value where there is a point of inflexion in F, a t-type distortion corresponds to moving away from the saddle point along an equipotential.

Limited studies of the neighborhood of the family of saddle-point shapes were made, as regards both symmetric and asymmetric distortions. For small symmetric deviations we may write the additional distortion energy $\xi - \xi_{sp}$ as

$$\xi - \xi_{sp} = ax^2 + by^2 + cz^2 + 2dyz + 2exz + 2fxy,$$

where

$$x = a_2 - a_2^{sp},$$
$$y = a_4 - a_4^{sp},$$
$$z = a_6 - a_6^{sp},$$

and a, b, c, d, e, and f are functions of u.

The expression for $\xi - \xi_{sp}$ may be thought of as an equation of a family of equipotential surfaces of second degree. For u close to 0 they are families of hyperboloids centered at the point $x = y = z = 0$.

A change of coordinates,

$$x' = kx + ly + mz,$$

$$y' = ux + vy + wz,$$

$$z' = px + qy + rz,$$

may be used to transform to principal axes, so that $\xi - \xi_{sp}$ becomes

$$\xi - \xi_{sp} = \lambda_2 x'^2 + \lambda_4 y'^2 + \lambda_6 z'^2 .$$

The eigenvalues λ_2, λ_4, λ_6 are found by solving the determinant

$$\begin{vmatrix} a - \lambda & f & e \\ f & b - \lambda & d \\ e & d & c - \lambda \end{vmatrix} = 0.$$

They may be used to study the "stiffness" of the saddle-point shapes against the distortions corresponding to displacements along the principal axes whose orientations in a_2, a_4, a_6 space, as given by the direction cosines klm, uvw, pqr, may be found by standard methods. The usual procedure of solving to successive powers in u gave the following expansions:

$$\lambda_2 = - 0.399995u - 0.476892u^2 + 6.830759u^3 + 4.221224u^4 + \ldots ,$$

$$\lambda_4 = 0.629630 - 0.303030u - 7.064607u^2 + \ldots .$$

$$\lambda_6 = 1.242604 + \ldots .$$

The functions λ_2 and λ_4 are plotted in Fig. 15.

8. Asymmetric Distortions

Consider the energy associated with an asymmetric distortion specified by a_1, a_3, a_5, a_7 around the symmetric saddle-point shape. For small distortions the problem again reduces to the study of equipotential surfaces of second degree, this time in four dimensions and with four principal axes. Along one of these axes, the one associated with a shift of the center of mass without intrinsic change of shape, the energy is found to be constant. The equipotential surfaces are therefore four-dimensional cylinders with three-dimensional cross sections in the form of ellipsoids or hyperboloids. (For $x = 1$ the axis of the cylinders is the a_1 axis. For $x < 1$ the axis points in some general direction in a_1, a_3, a_5, a_7 space. The constancy of the

energy along this axis would be exact in a many-dimensional space with all the a_n's displayed; in a limited subspace like the one we are considering the constancy holds only up to a certain order in u).

Instead of studying the equipotential surfaces in four dimensions we may restrict ourselves to a study of a suitable section of the cylinder by a three-dimensional hyperplane in four dimensions. Two cases are considered. In the first the plane is taken at right angles to the axis of the cylinder, so as to contain the remaining three principal axes. The stiffness of the system against distortions along these principal axes may then be studied as before.

The second case corresponds to studying a section of the four-dimensional cylinder by a hyperplane so oriented that points within this plane correspond to distortions that leave the center of mass of the drop at the origin. Contrary to what was expected, the normal to this plane does not coincide with the direction of the axis of the four-dimensional cylinder (representing pure shifts of the center of mass), except in the case x = 1, when the saddle-point shape is a sphere. As x decreases below 1 the two directions diverge at a rate proportional at first to (1-x). The ellipsoidal or hyperboloidal families of three-dimensional surfaces defined by the new section of the cylinder are therefore not identical with the previously mentioned family containing the principal axes.

We illustrate the second case first. It may be verified that taking a section of the four-dimensional cylinder by the "constant-center-of-mass plane" and then projecting the resulting three-dimensional figures from the space defined by the section onto the three-dimensional space of the a_3, a_5, and a_7 coordinates corresponds, algebraically, to using the expressions for the deformation energy in which a_1 has been eliminated by the center-of-mass condition (Eqs. (14) and (15)). The result may be written

$$\xi - \xi_{sp} = a a_3^2 + b a_5^2 + c a_7^2 + 2d a_5 a_7 + 2e a_3 a_7 + 2f a_3 a_5 ,$$

where a, b, c, d, e, f are functions of u (different from the functions of Section 7). Diagonalization of this expression led to the following expansion for the eigenvalue λ_3 (which belongs to a_3 in the sense that it reduces to the coefficient of a_3^2 in the limit $u \to 0$):

$$\lambda_3 = 0.306122 - 0.353739u - 3.206288u^2 + 7.442375u^3 - (3.837496)u^4 + \ldots .$$

This result is plotted in Fig. 16. The last term is not the exact coefficient of u^4, because one of the combinations of a_n's necessary for its evaluation was not available.

As an illustration of the more direct procedure, in which the diagonalization is carried out without the elimination of α_1, we present the results of a more restricted calculation in which α_6 and α_7 were not included, and the expression

$$\xi - \xi_{sp} = a\alpha_1^2 + b\alpha_3^2 + c\alpha_5^2 + 2d\alpha_3\alpha_5 + 2e\,\alpha_1\alpha_5 + 2f\alpha_1\alpha_3$$

was brought to principal axes. The functions a, b, c, d, e, f (not the same as before) are given explicitly by

$$a = 0.0 + 0.0u + 2.400000u^2 + \dots ,$$

$$b = 0.306122 - 0.353739u - 4.770074u^2 + 9.009821u^3 + 37.569611u^4 + \dots ,$$

$$c = 0.942149 - 0.262770u - 12.415024u^2 + \dots ,$$

$$d = 0.0 - 0.983864u + 0.119320u^2 + 2.218091u^3 + \dots ,$$

$$e = 0.0 + 0.0u + 1.547881u^2 + \dots ,$$

$$f = 0.0 - 0.857142u - 0.281225u^2 + 10.455021u^3 + \dots .$$

The eigenvalues λ_1, λ_3, λ_5 were found to be given by

$$\lambda_1 = 0.0 + 0.0u + 0.0u^2 ,$$

$$\lambda_3 = 0.306122 - 0.353739u - 3.892004u^2 + 13.944823u^3 + 6.586599u^4 ,$$

$$\lambda_5 = 0.942149 - 0.262770u - 10.893095u^2 .$$

Some of the higher-order terms in the above expressions would be affected by the inclusion of further combinations of α's in the energy expansions.

In the space of α_1, α_3, α_5 the orientation of the "pure center-of-mass shift" axis was found to be specified to lowest order in u, by the following unnormalized direction cosines (1.0, 2.800000u, 0.0u). This is the direction along which the energy is constant; it may be verified directly, by a purely geometrical re-expansion of the symmetric shape about an axially displaced origin, that this is indeed the direction of an over-all center-of-mass shift.

The unnormalized direction cosines of the normal to the "constant-center-of-mass plane" are given to lowest order in u, by (1.0, 1.800000u, 0.0u).

The above examples are meant as illustrations of the methods that may be used in a systematic mapping of the potential energy of a charged drop. As regards quantitative results it would seem that for

x values below about x = 0.8 expansions about spheroids rather than spheres are necessary. In the case of the threshold energy, however, the sixth-order expansion in (1-x) would appear to be remarkably accurate down to x = 0.7 or perhaps even lower. This may be associated with the fact that the threshold energy, unlike the other quantities for which power expansions have been considered, is invariant with respect to the choice of distortion coordinates, and its rate of convergence in an expansion in powers (1-x) is governed by the criterion $(1-x) \ll 1$, rather than by the related but not identical criterion $\alpha_n \ll 1$.

ACKNOWLEDGMENTS

The work reported in this paper was begun in 1956 at the Institute for Mechanics and Mathematical Physics and The Gustaf Werner Institute for Nuclear Chemistry, Uppsala, Sweden. I should like to thank Professors I. Waller and T. Svedberg for the hospitality of their Institutes.

A large part of the work was carried out during a stay in 1956 - 1957 at the Institute of Physics, Aarhus University, Denmark, and I should like to thank my friends there, and especially Jens Lindhard and Pablo Kristensen, for the inspiring atmosphere and excellent working conditions of their Institute.

It is a pleasure to acknowledge the hospitality of the Radiation Laboratory, University of California, and the many discussions with my colleagues in both the Chemistry and Theoretical Physics Divisions.

APPENDIX

Some of the coefficients $(pqr) = \int_{-1}^{1} P_p P_q P_r \, d\xi$, supplementing the more restricted table of Ref. 2 are given below.

$(156) = 12/143$
$(167) = 14/195$
$(178) = 16/255$

$(277) = 112/3315$
$(279) = 72/1615$

$(347) = 70/1287$
$(356) = 14/429$
$(358) = 112/2431$
$(367) = 336/12155$
$(378) = 504/20995$
$(3,7,10) = 80/2261$

$(457) = 560/21879$
$(477) = 4536/230945$

$(556) = 160/7293$
$(558) = 980/46189$
$(5, 5, 10) = 1512/46189$
$(567) = 840/46189$
$(578) = 720/46189$
$(5, 7, 10) = 1540/96577$
$(5, 7, 12) = 4752/185725$

REFERENCES

1. W. J. Swiatecki, Deformation Energy of a Charged Drop. I. Qualitative Features, Phys. Rev., 101:651 (1956).
2. W. J. Swiatecki, Deformation Energy of a Charged Drop. II. Symmetric Saddle-Point Shapes, Phys. Rev. 104:993 (1956).
3. V. G. Nossoff, Report A/CONF, 8/P/653 U. S. S. R., from the 1955 Geneva Conference on the Peaceful Uses of Atomic Energy (United Nations, New York, 1956).
4. D. H. Hill and J. A. Wheeler, Nuclear Constitution and the Interpretation of Fission Phenomena, Phys. Rev. 89:1102 (1953).
5. N. Bohr and J. A. Wheeler, The Mechanism of Nuclear Fission, Phys. Rev. 56:426 (1939).
6. C. Maxwell, Article on "Capillary Action" (revised by Lord Rayleigh) in the 11th Edition of the Encyclopaedia Britannica (1910).
7. U. L. Businaro and S. Gallone, On the Interpretation of Fission Asymmetry according to the Liquid-Drop Nuclear Model, Nuovo cimento, 1:629 (1955).
8. U. L. Businaro and S. Gallone, Saddle Shapes, Threshold Energies and Fission Asymmetry on the Liquid-Drop Model, Nuovo cimento, 1:1277 (1955).
9. W. R. Smythe, Static and Dynamic Electricity, McGraw-Hill Co., Inc., New York (1939).
10. N. Mudd, The Gravitational Potential and Energy of Harmonic Deformations of any Order, Messenger of Mathematics, 40:137 (1910-11).
11. W. J. Swiatecki, The Density Distribution inside Nuclei and Nuclear Shell Structure, Proc. Phys. Soc. (London), 63A:1208 (1950).
12. S. Frankel and N. Metropolis, Calculations In the Liquid-Drop Model of Fission, Phys. Rev. 72:914 (1947).
13. H. Lamb, Hydrodynamics, Dover Publications, New York (1945).

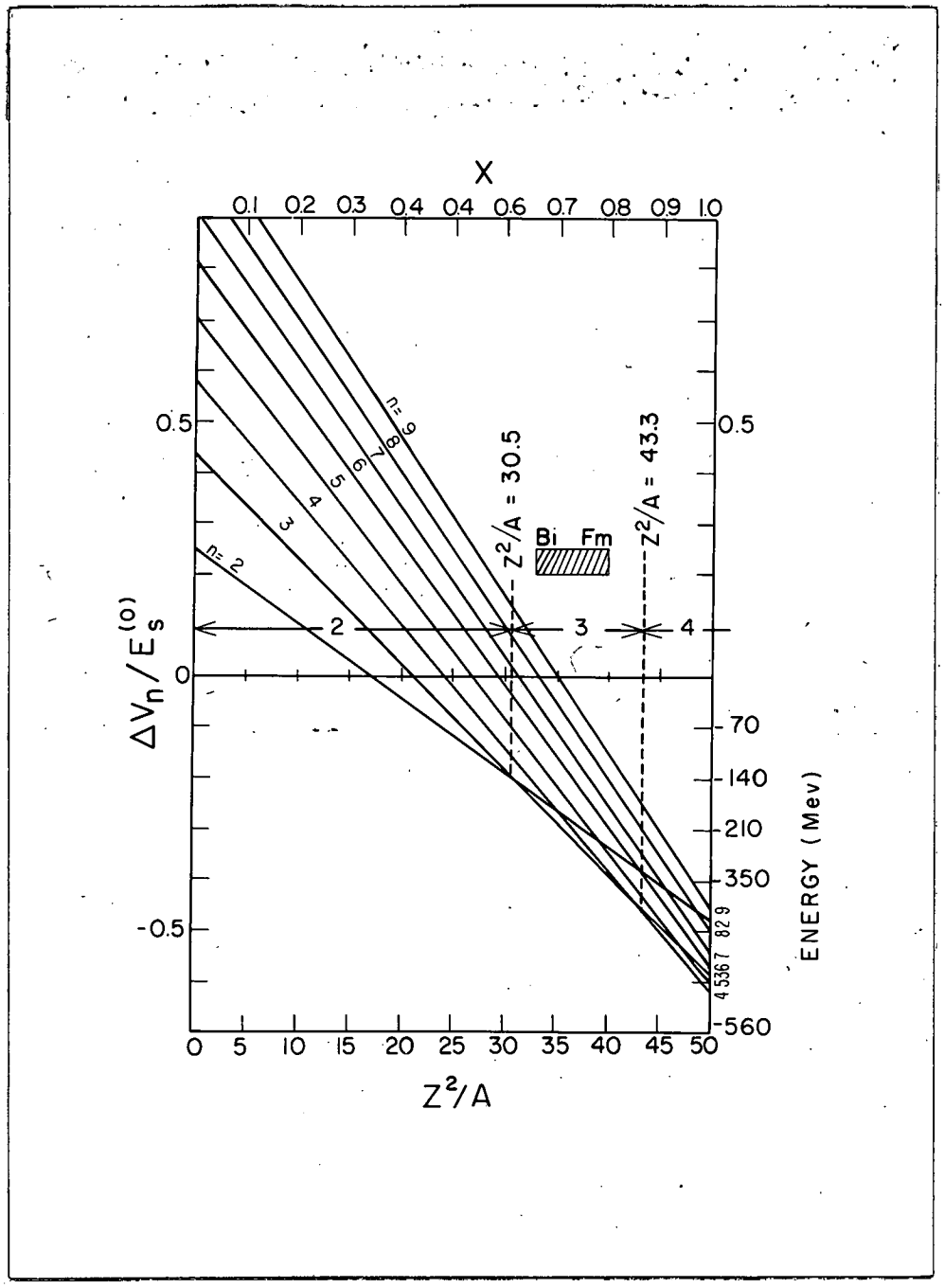

Fig. 1. The energy released in the division of a drop into n equal parts, as function of the fissionability parameter x.

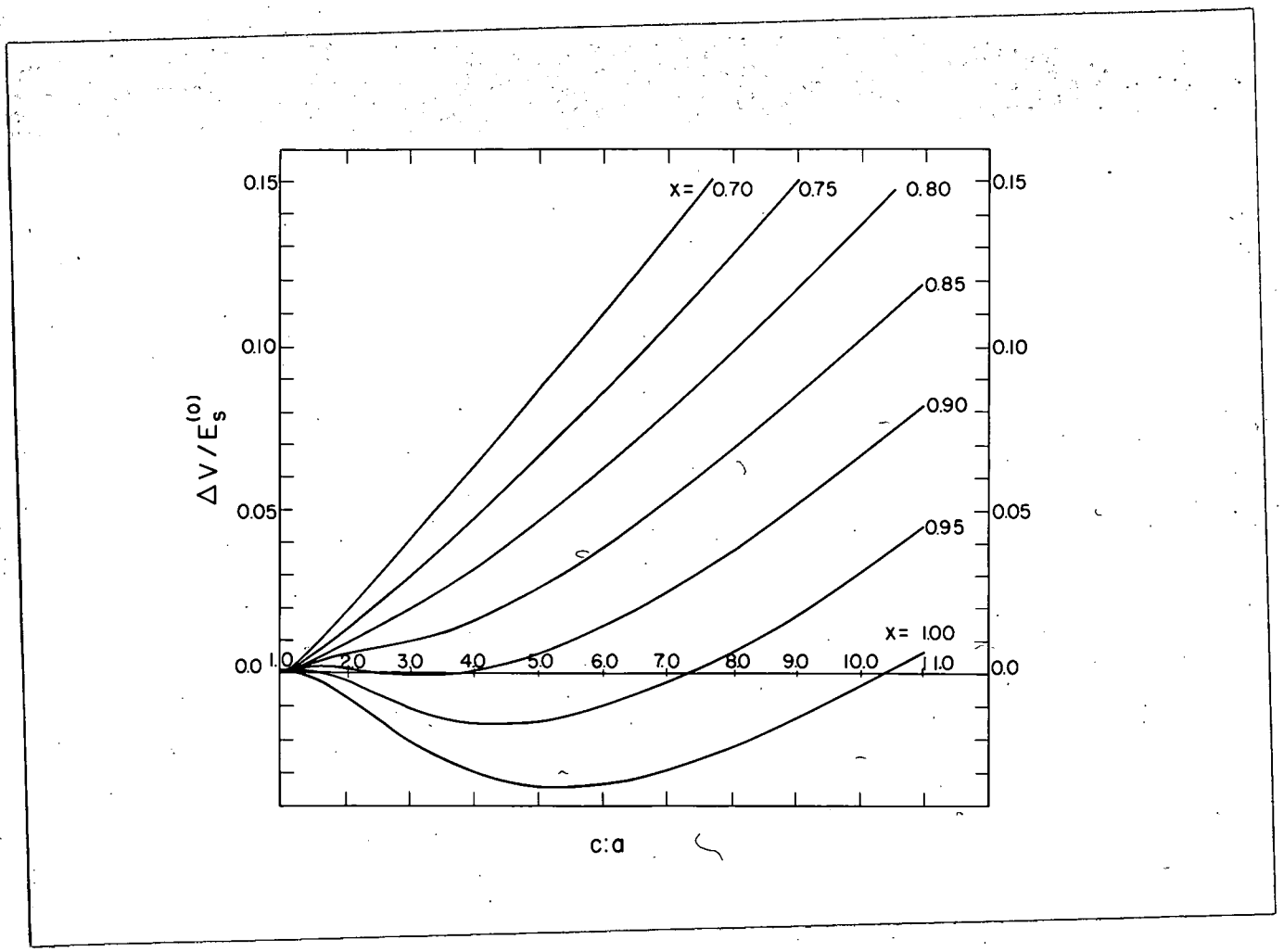

Fig. 2. The deformation energy for spheroidal distortions as function of the ratio of axes, for different values of x. The unit of energy in this and the following figures is $E_s^{(0)}$, the surface energy of the undistorted drop.

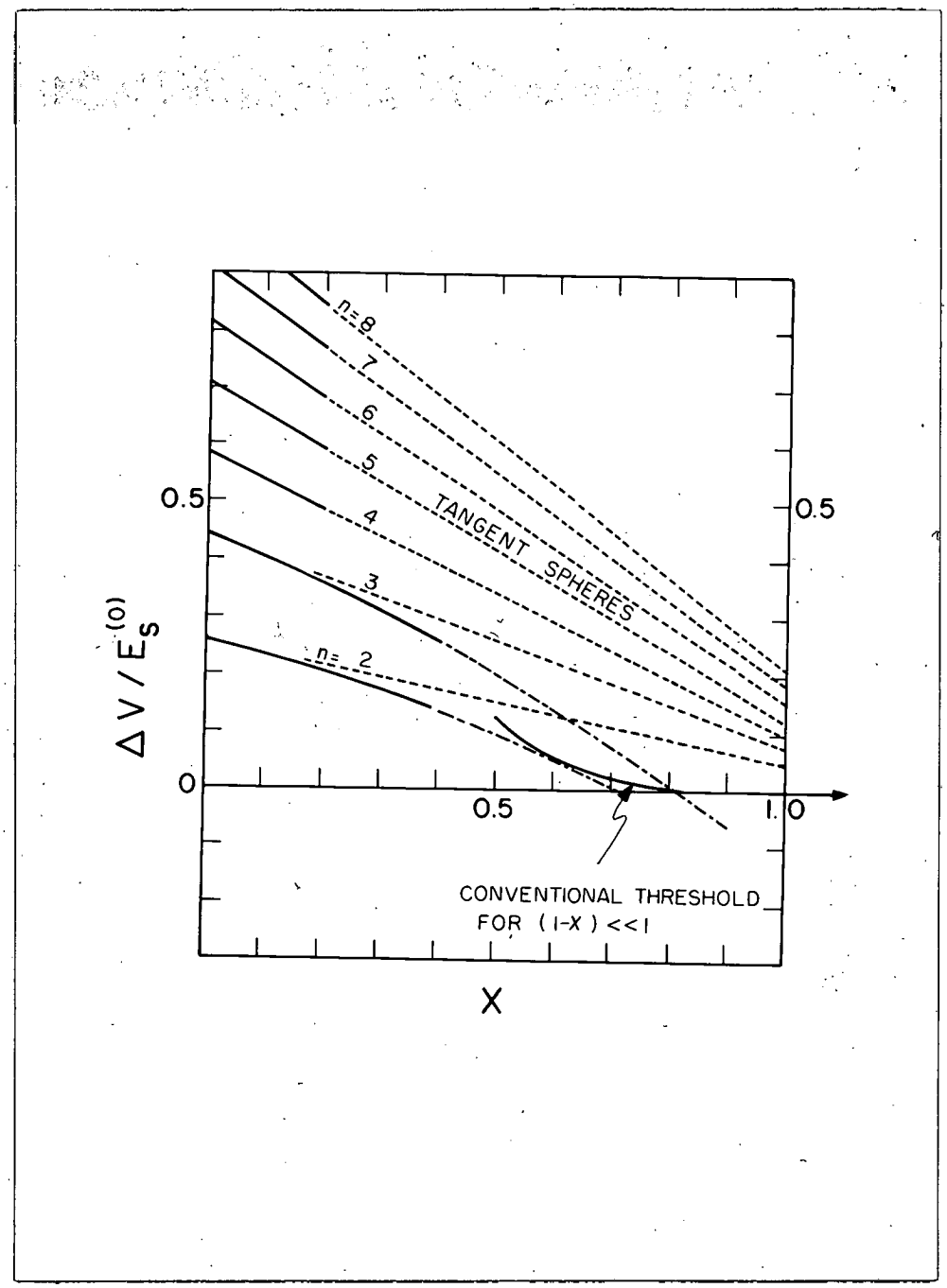

Fig. 3. The energies of families of saddle-point shapes for $x \ll 1$ and the energy of the conventional threshold for $x \to 1$. The dotted lines correspond to the first-order approximation, the dot-dash curves correspond to an estimate of the second-order approximation.

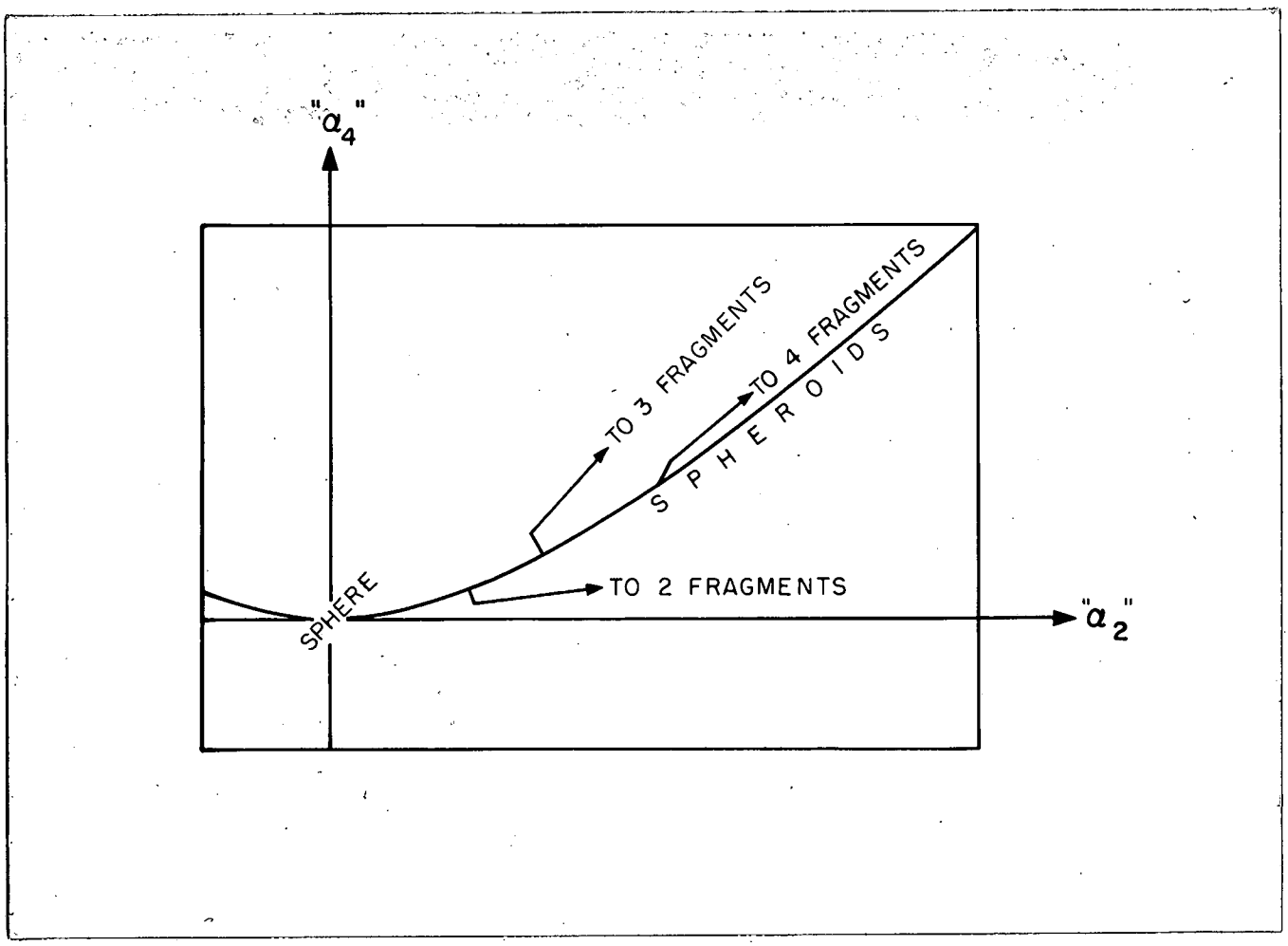

Fig. 4. An attempt to illustrate schematically the relation of the potential-energy valleys associated with divisions into different numbers of fragments to the locus of spheroidal distortions in the space of deformation coordinates specifying the shape of the drop.

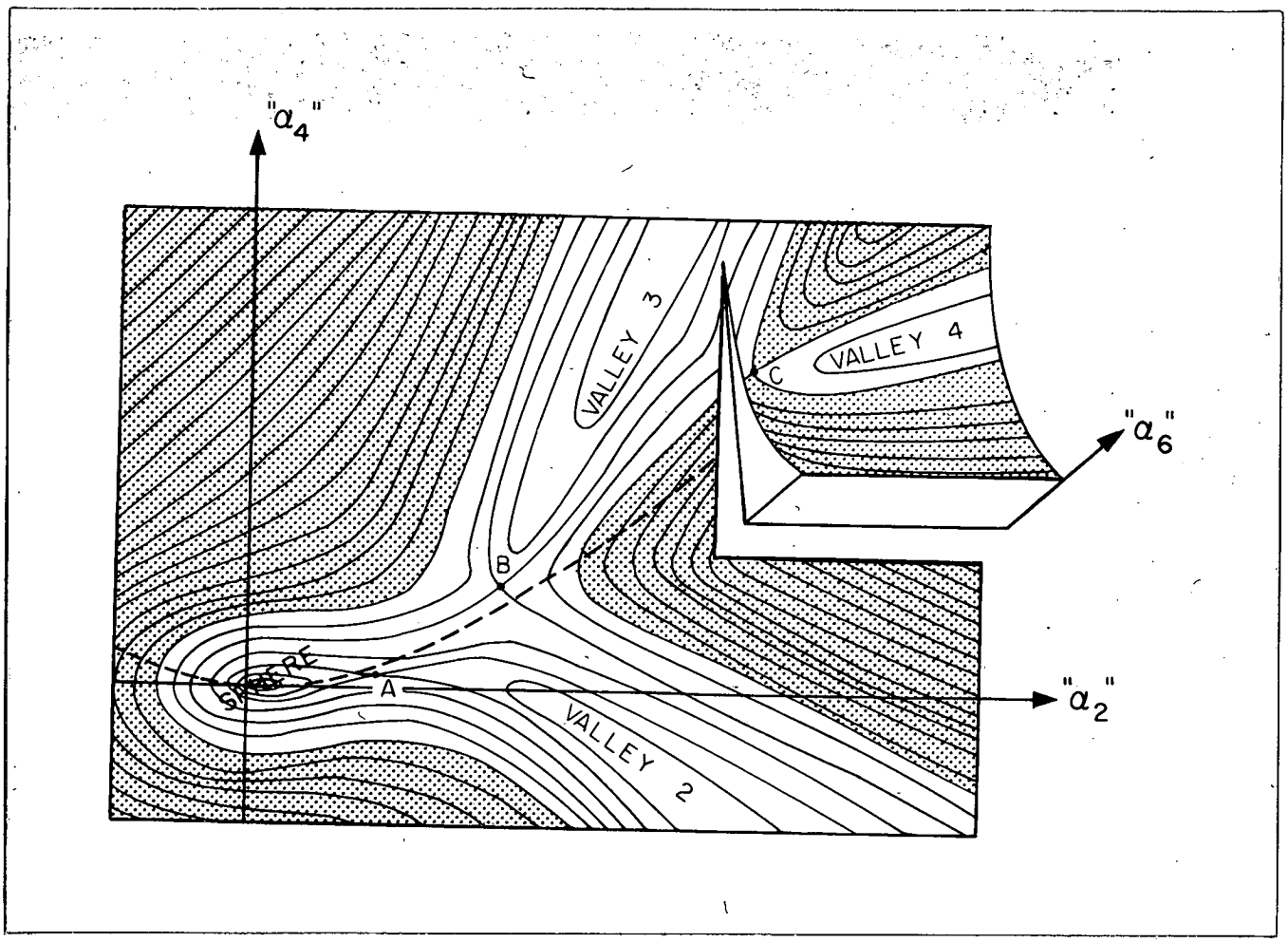

Fig. 5. A schematic map of several potential-energy valleys separated from one another and from the hollow around the spherical configuration by saddle points A, B, C. The map corresponds to the case when the energies of the saddles are in the order $E(A) < E(B) < E(C)$. The dashed line represents the locus of spheroidal distortions.

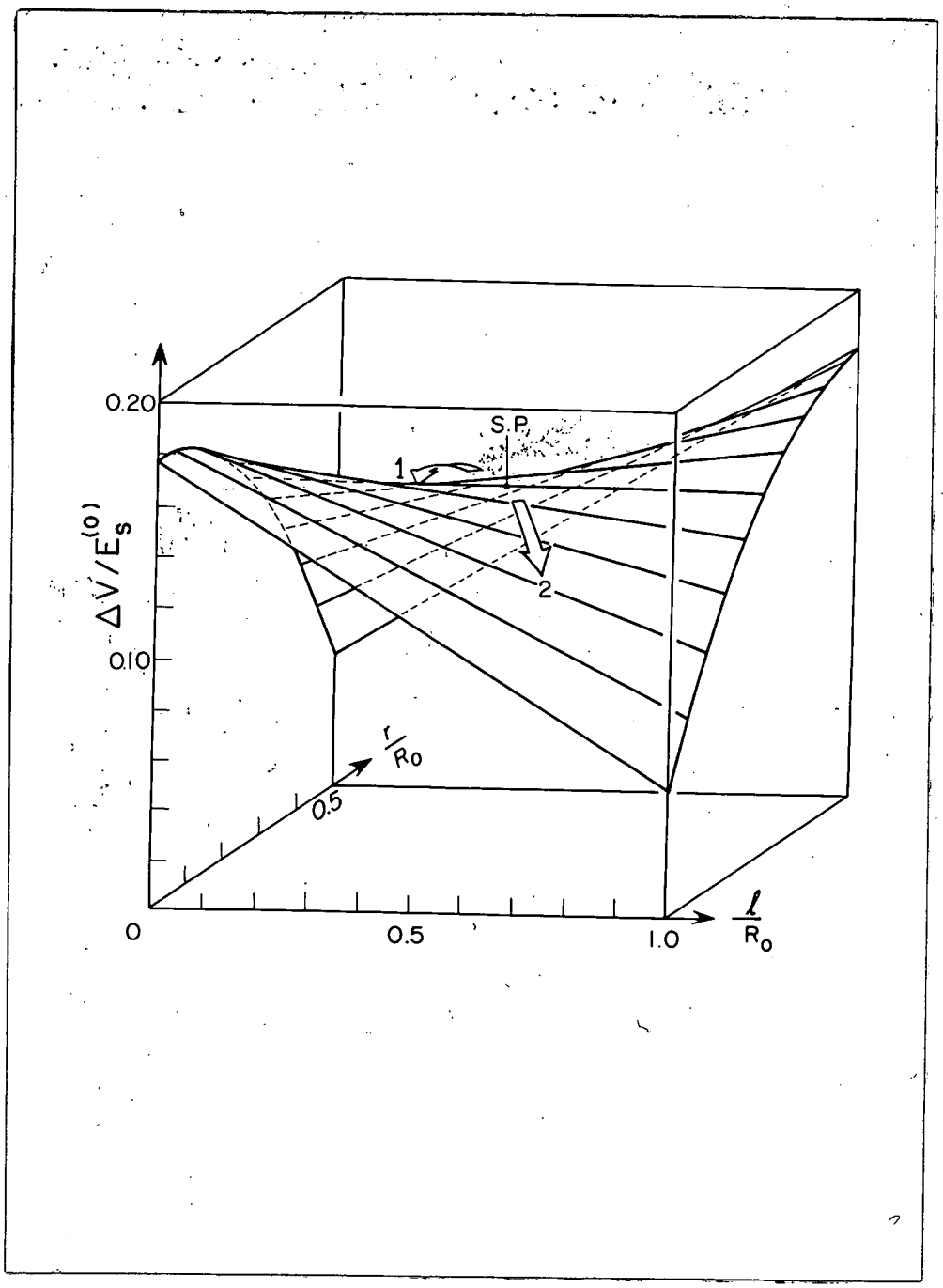

Fig. 6. The deformation energy of the symmetrical configuration of two equal spherical fragments connected by a small cylindrical neck of length ℓ and radius r, plotted as function of r/R_0 and ℓ/R_0, where R_0 is the radius of the original sphere. An expression valid approximately for $x \ll 1$ was used, with the value $x = 0.384$ inserted in the equation. The saddle point is indicated by an arrow and the directions leading to the one- and two-fragment valleys are shown.

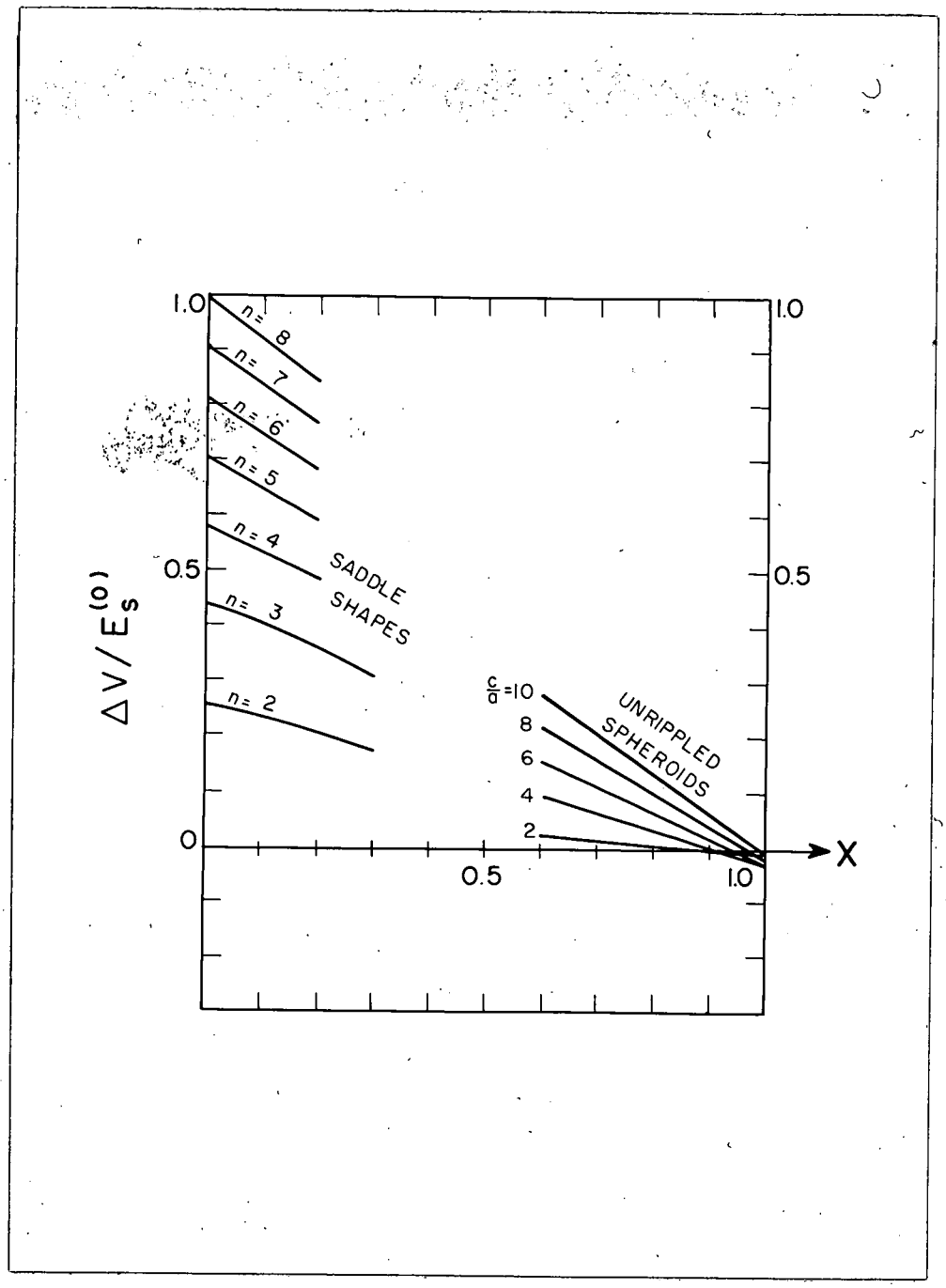

Fig. 7. Threshold energies for x << 1 and the deformation energies of spheroids with various ratios of semi-axes, c: a, plotted as functions of x.

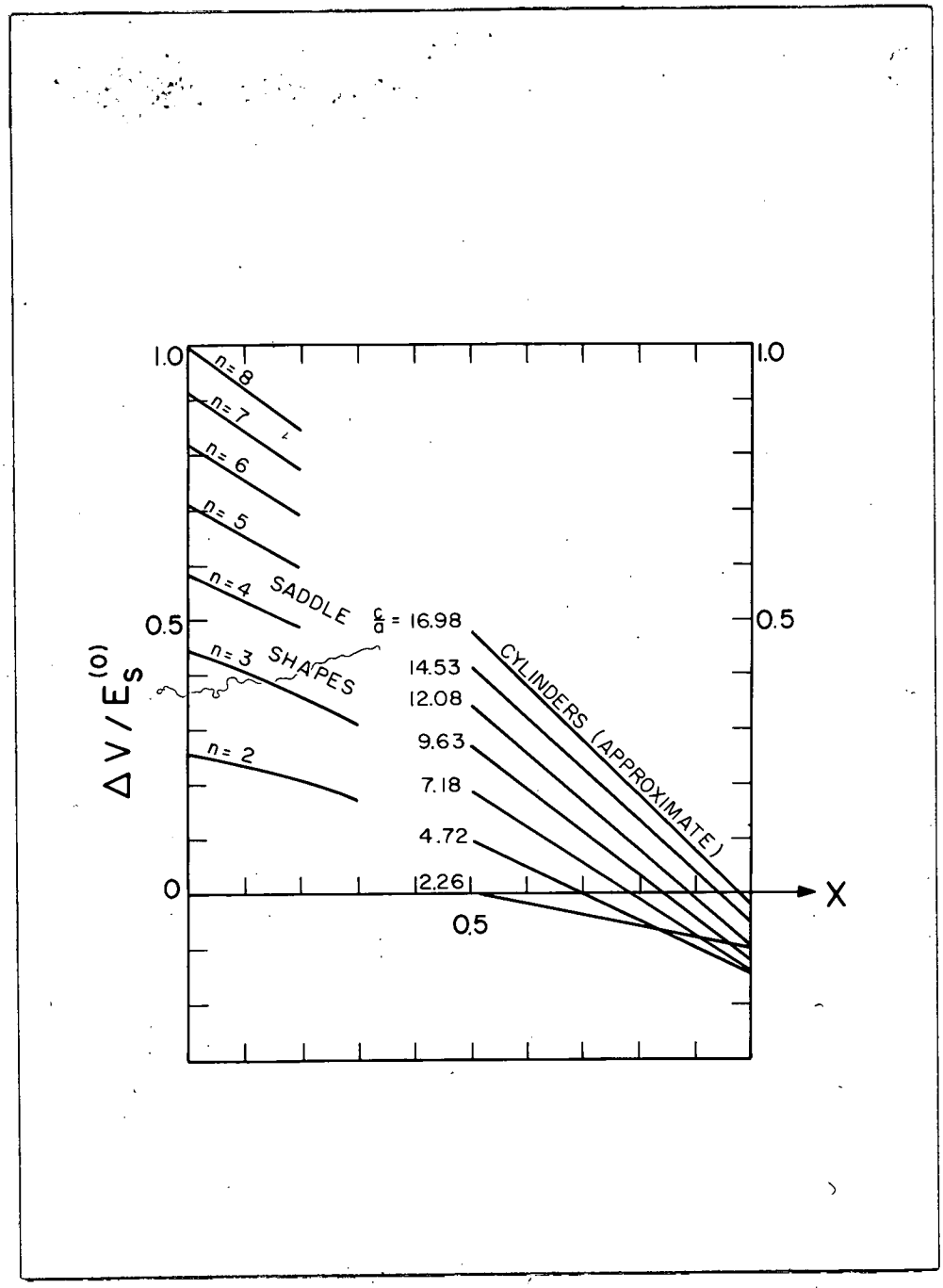

Fig. 8. Threshold energies for $x \ll 1$ and the estimated deformation energies of cylinders with hemispherical ends, for different ratios of the semi-axes, c: a. The surface energies are exact but the electrostatic energies of the cylinders were estimated by replacing them with strings of 2, 4, 6, 8, 10, or 12 tangent spheres with the same volume and the same over-all length 2c. (Hence the sequence of fractional ratios c: a.)

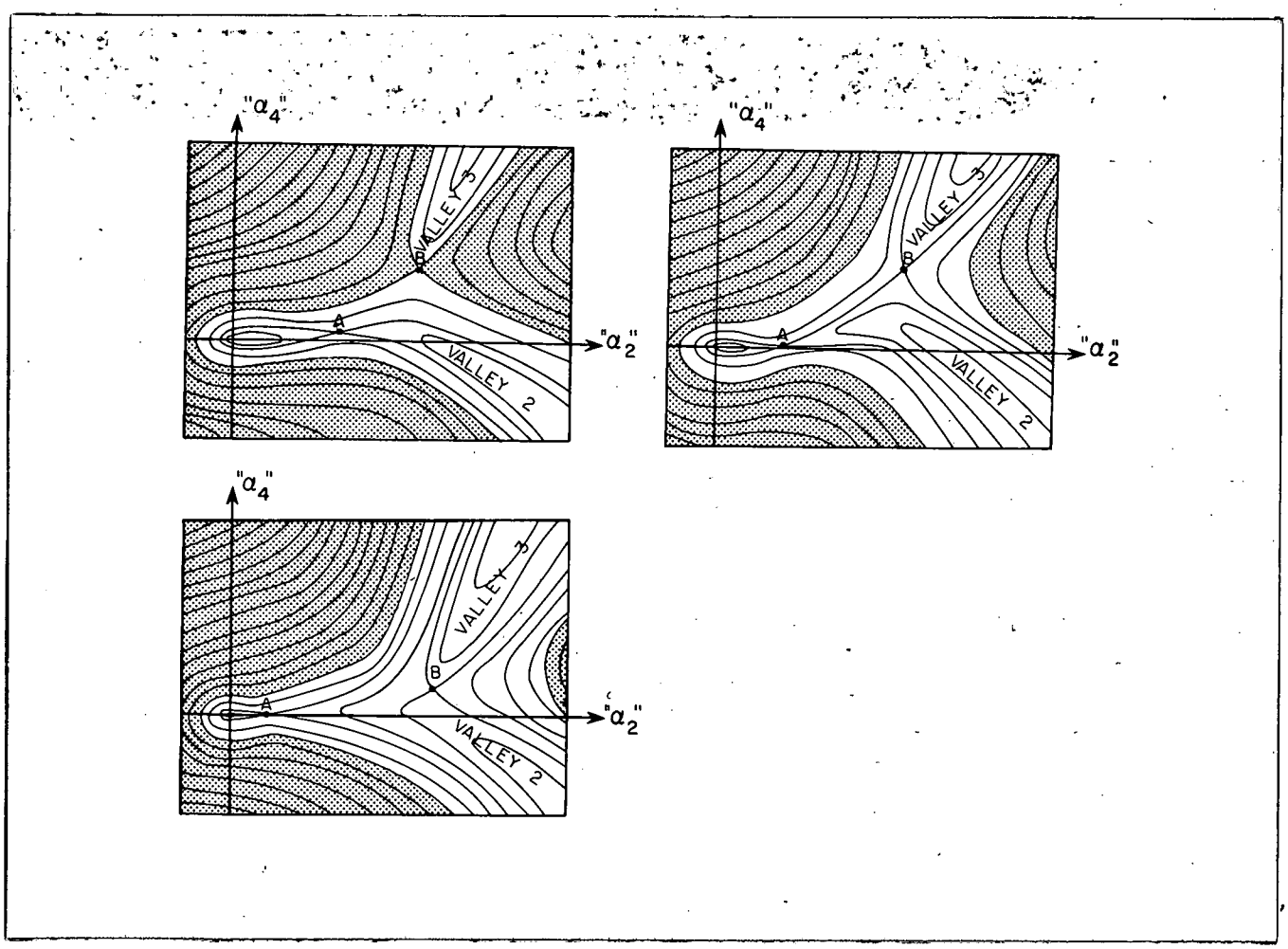

Fig. 9. Three maps showing schematically the relations between the two- and three- fragment valleys for different values of x. In (a) the threshold B is higher than A, $E(B) > E(A)$, and low-energy fission must proceed by way of the two-fragment valley. In (b) $E(B) = E(A)$ and in (c) $E(B) < E(A)$, and a competition between the two valleys would be involved.

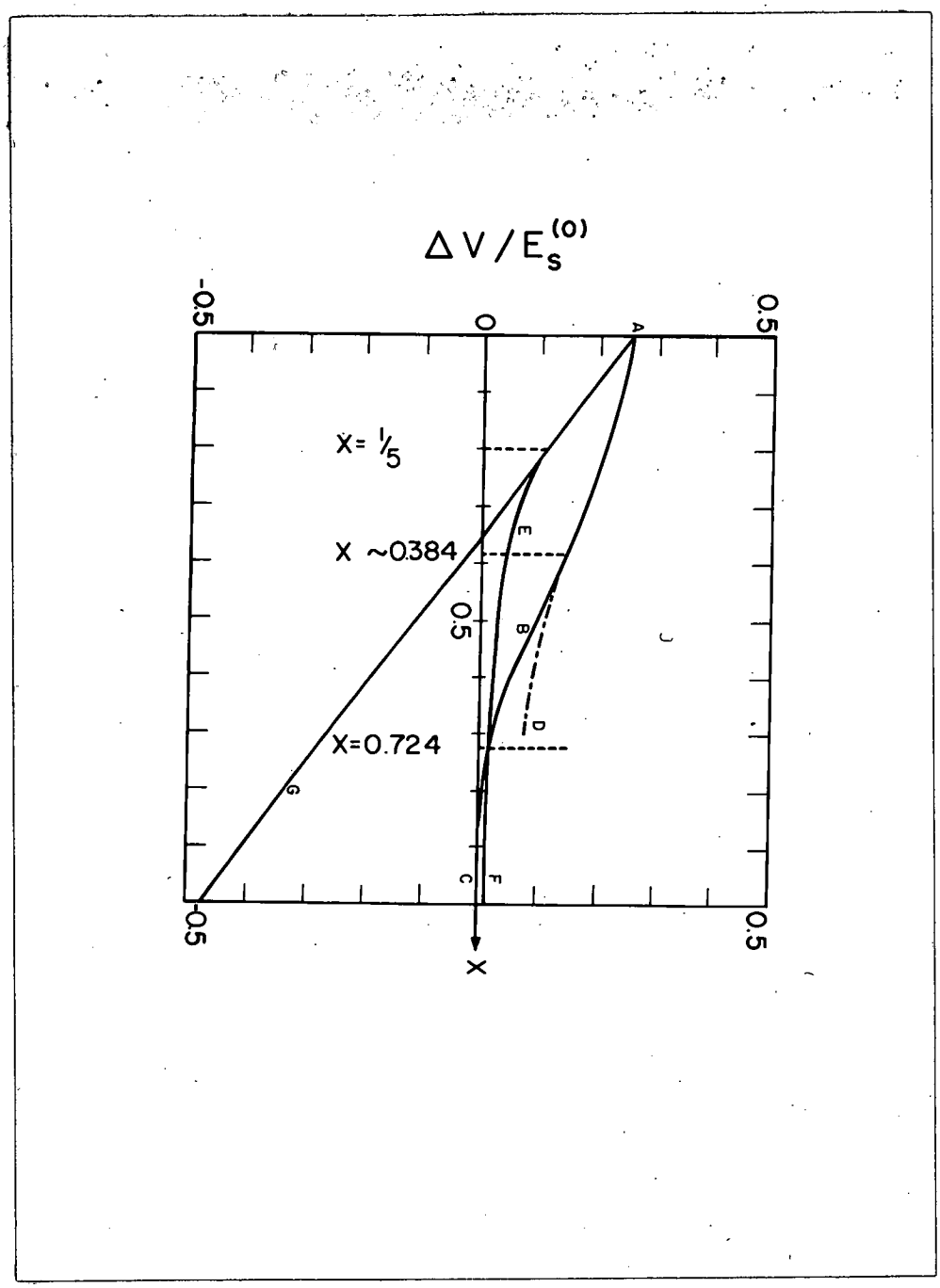

Fig. 10. The energies of two symmetric and two asymmetric families of equilibrium shapes (in units of $E_s^{(0)}$) plotted as functions of x. The line AG refers to two equal spherical fragments at infinity (compare Fig. 1). Beyond the point of bifurcation at $x = 1/5$ two unequal fragments at infinity also have an energy stationary with respect to all deformations - this energy is shown by the curve EF. The curve ABC is the conventional threshold (interpolated on the assumption that the curve for $x \to 1$ goes over into the curve for $n = 2$ when $x \ll 1$). Beyond the estimated point of bifurcation at $x \sim 0.38$ an asymmetric configuration of equilibrium with energy given by the curve D appears. The curves EF and BC intersect at $x = 0.724$.

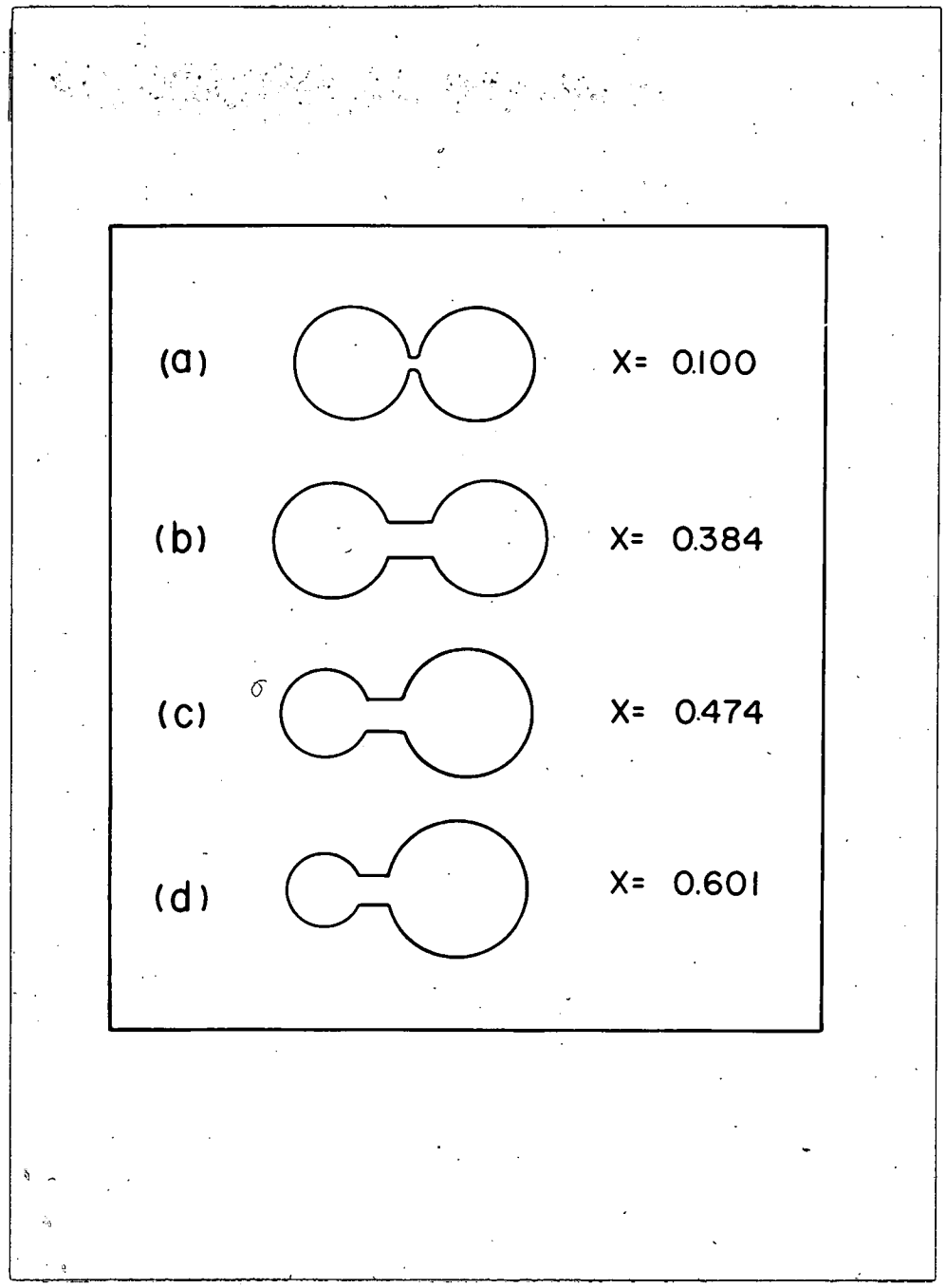

Fig. 11. Configurations of equilibrium estimated by making the energy stationary for a restricted family of shapes consisting of two spheres joined by a cylindrical neck. A further approximation was the use of an expression for the energy that is valid only when the neck is small. The cases (a) and (b) refer to the symmetric saddle point shapes. Beyond $x \sim 0.38$ asymmetric equilibrium shapes illustrated by (c) and (d), appear. The energies of the shapes (a), (b), (c), (d) are given by the curve AD in Fig. 10.

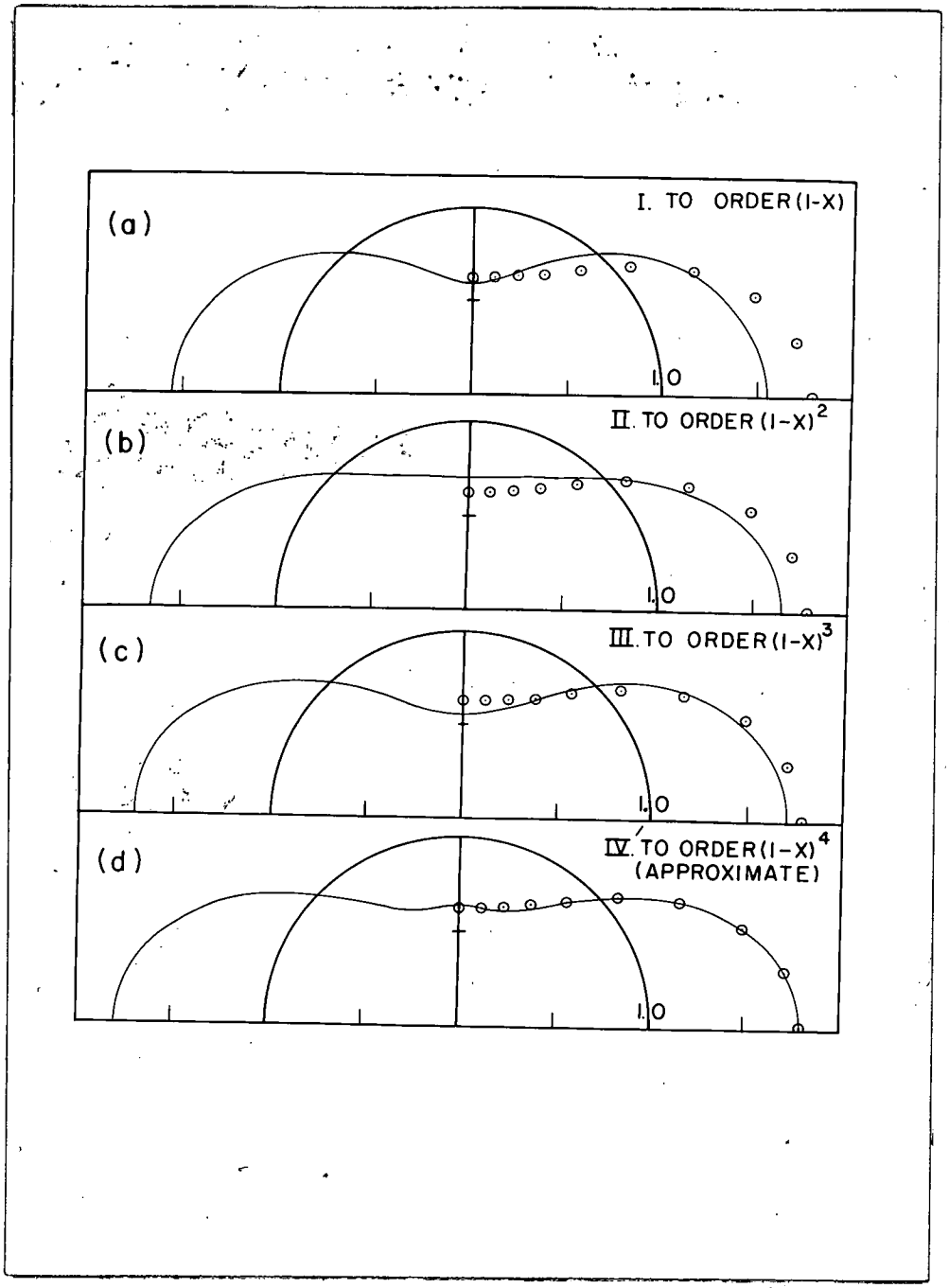

Fig. 12. The conventional saddle-point shape for x = 0.7, as calculated in four approximations using an expansion about the spherical shape. The circles refer to the saddle-point shape calculated in Ref. 2, based on expansions about spheroids. The last figure, (d), is not the exact result to fourth order in (1-x): with the available expansion coefficients, a_2^{sp} and a_4^{sp} could be calculated to order $(1-x)^4$, but a_6^{sp} only to order $(1-x)^3$ and a_8^{sp} was not included at all, although it would be of order $(1-x)^4$.

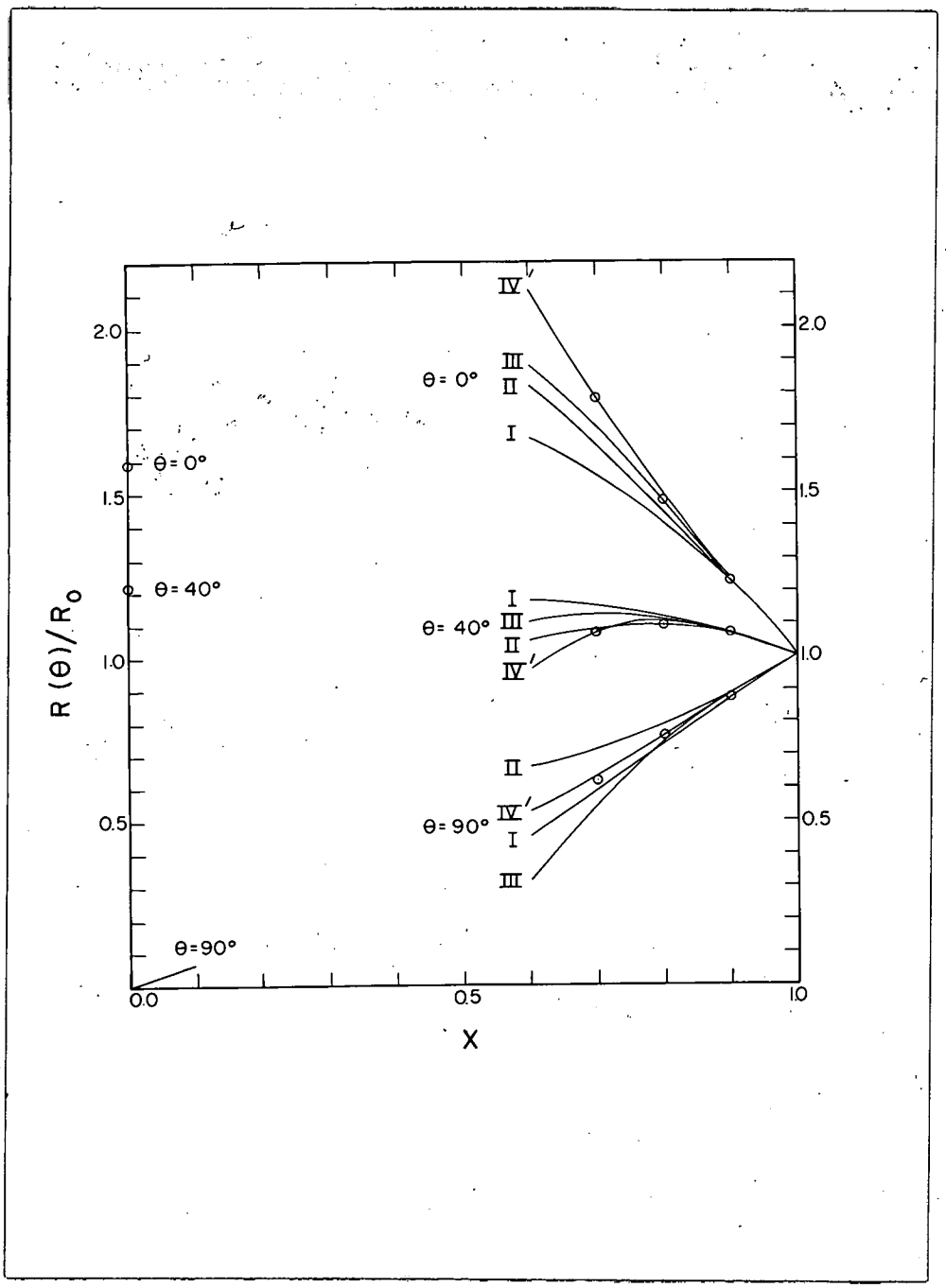

Fig. 13. The radius vectors of saddle-point shapes (in units of R_0) plotted against x for $\theta = 0^\circ$, 40°, 90°. The four sets of curves labeled I, II, III, IV' refer to calculations to order (1-x), $(1-x)^2$, $(1-x)^3$ and $(1-x)^4$, but the last one suffers from the limitations mentioned under Fig. 10. The points on the right are from expansions about spheroids, Ref. 2.

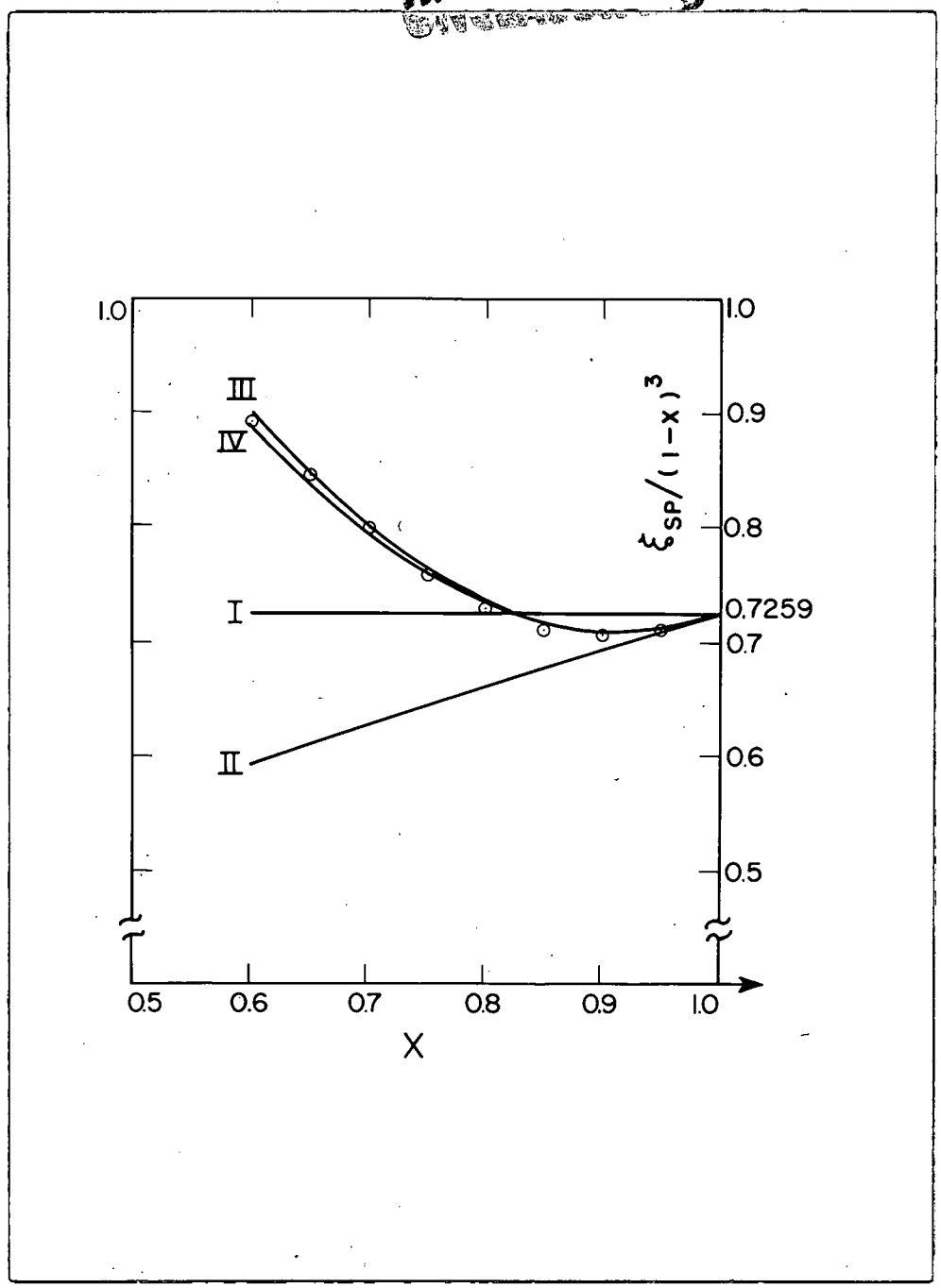

Fig. 14. The energy of the conventional threshold (in units of $E_s^{(0)}$ and divided by $(1-x)^3$), plotted against x. The four curves labeled I, II, III, and IV correspond to expansions for the threshold to order $(1-x)^3$, $(1-x)^4$, $(1-x)^5$, and $(1-x)^6$. The coefficients of all terms, including the last, are exact. The circles are from Ref. 2; in the range of x values from 0.6 to 1.0 they differ from the fifth- or sixth-order curves by less than $1\frac{1}{2}\%$.

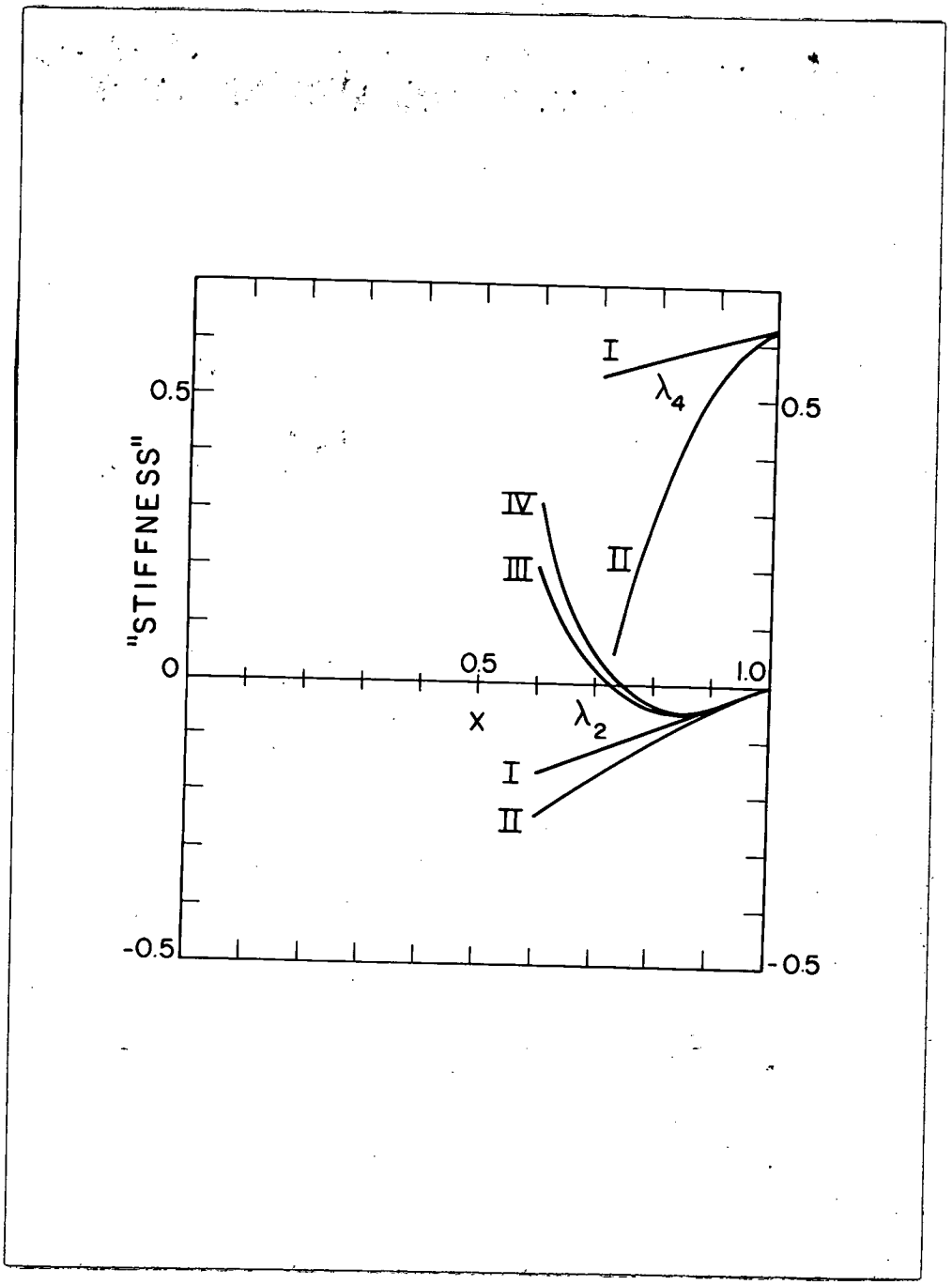

Fig. 15. The stiffnesses λ_2 and λ_4 of the conventional saddle-point shape against distortions along two of the principal axes in α_2, α_4, α_6 space, plotted against x in different orders of approximation: to first, second, third, and fourth powers of (1-x) in the case of λ_2 and to the first and second powers of (1-x) in the case of λ_4.

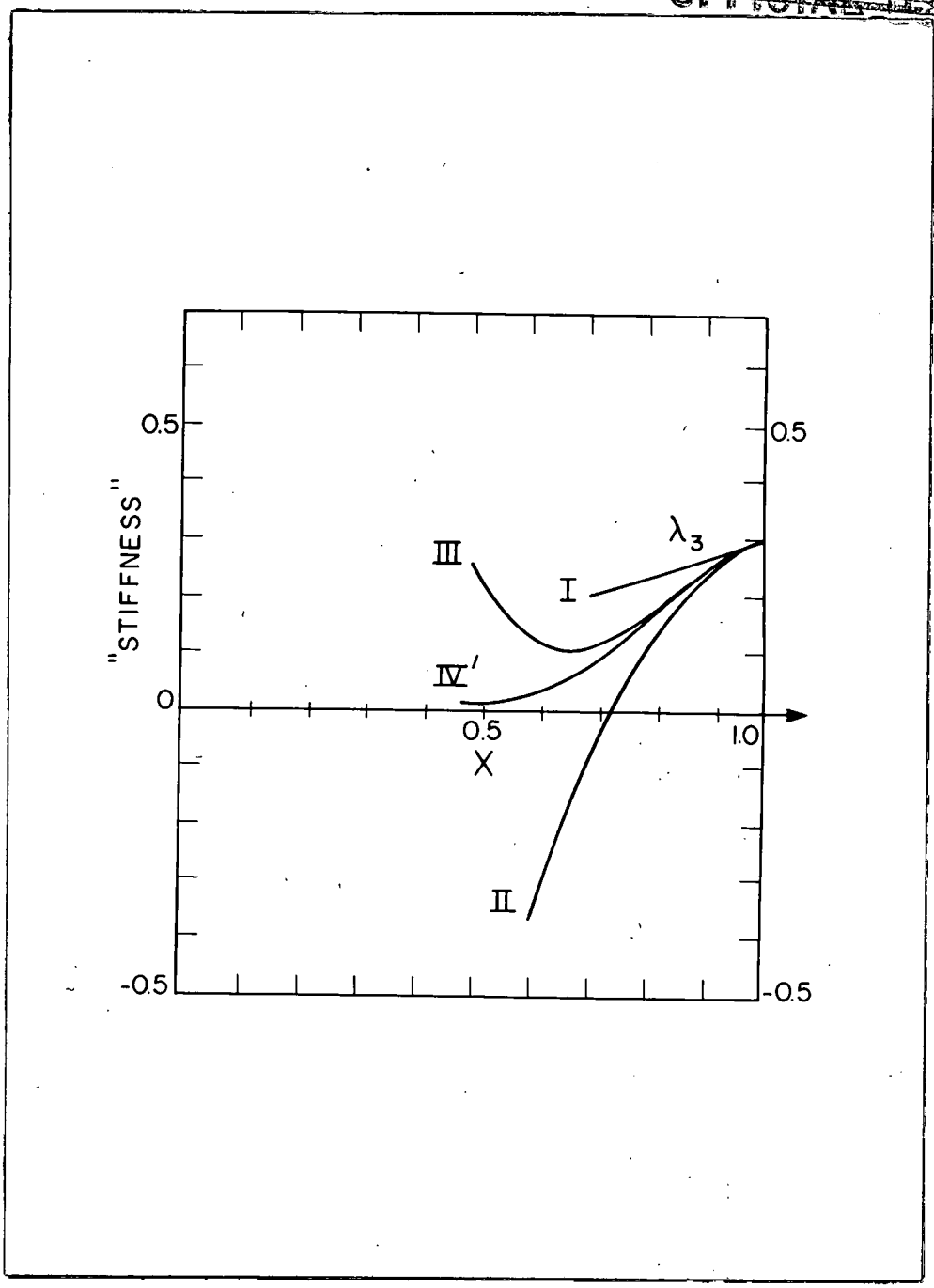

Fig. 16. The stiffness of the conventional saddle-point shape associated with a distortion along a principal axis in a_3, a_5, a_7 space (see text for a more precise definition of λ_3). The same remarks as in the legend to Fig. 13 apply to the four orders of approximation labeled by I, II, III, and IV'.